



Deposited via The University of Leeds.

White Rose Research Online URL for this paper:

<https://eprints.whiterose.ac.uk/id/eprint/122960/>

Version: Accepted Version

---

**Article:**

Kottke, T, Evgin, L, Shim, KG et al. (2017) Subversion of NK-cell and TNF $\alpha$  Immune Surveillance Drives Tumor Recurrence. *Cancer Immunology Research*, 5 (11). pp. 1029-1045. ISSN: 2326-6066

<https://doi.org/10.1158/2326-6066.cir-17-0175>

---

© 2017, American Association for Cancer Research. This is an author produced version of a paper published in *Cancer Immunology Research*. Uploaded in accordance with the publisher's self-archiving policy.

**Reuse**

Items deposited in White Rose Research Online are protected by copyright, with all rights reserved unless indicated otherwise. They may be downloaded and/or printed for private study, or other acts as permitted by national copyright laws. The publisher or other rights holders may allow further reproduction and re-use of the full text version. This is indicated by the licence information on the White Rose Research Online record for the item.

**Takedown**

If you consider content in White Rose Research Online to be in breach of UK law, please notify us by emailing [eprints@whiterose.ac.uk](mailto:eprints@whiterose.ac.uk) including the URL of the record and the reason for the withdrawal request.

1 **Subversion of NK Cell and TNF $\alpha$  Immune Surveillance Drives Tumor Recurrence**

2

3 Tim Kottke<sup>1</sup>, Laura Evgin<sup>1</sup>, Kevin G. Shim<sup>1</sup>, Diana Rommelfanger<sup>1</sup>, Nicolas Boisgerault<sup>1</sup>, Shane  
4 Zaidi<sup>1</sup>, Rosa Maria Diaz<sup>1</sup>, Jill Thompson<sup>1</sup>, Elizabeth Ilett<sup>2</sup>, Matt Coffey<sup>3</sup>, Peter Selby<sup>2</sup>, Hardev  
5 Pandha<sup>4</sup>, Kevin Harrington<sup>5</sup>, Alan Melcher<sup>5</sup>, Richard Vile<sup>1,2,6\*</sup>.

6

7 Running title: Treating tumor recurrence

8

9 Keywords: Immune responses to cancer, immunomodulation, tumor resistance to immune  
10 response

11

12 <sup>1</sup>Department of Molecular Medicine, Mayo Clinic, Rochester, MN 55905; <sup>2</sup>Leeds Institute of  
13 Cancer and Pathology, St. James' University Hospital, Leeds, UK; <sup>3</sup>Oncolytics Biotech  
14 Incorporated, Calgary, Canada; <sup>4</sup>University of Surrey, Guildford, UK; <sup>5</sup>The Institute of Cancer  
15 Research, 237 Fulham Road, London, SW3; <sup>6</sup>Department of Immunology, Mayo Clinic,  
16 Rochester, MN 55905

17

18 Funding: The European Research Council, The Richard M. Schulze Family Foundation, the  
19 Mayo Foundation, Cancer Research UK, the National Institutes of Health (R01 CA175386 and  
20 R01 CA108961), the University of Minnesota and Mayo Clinic Partnership and a grant from  
21 Terry and Judith Paul.

22

23 The authors have declared that no conflict of interest exists.

24

25 Word count: 5623; 7 figures, 0 supplementary figures, 2 tables

26

27 **Corresponding Author:** Richard G. Vile, Ph.D. / Mayo Clinic / Gugg 18 / 200 1<sup>st</sup> Street SW /

28 Rochester, MN 55905; 507-284-3178; vile.richard@mayo.edu

29 **Abstract**

30           Understanding how incompletely cleared primary tumors transition from minimal  
31 residual disease (MRD) into treatment resistant, immune-invisible recurrences has major clinical  
32 significance. We show here that this transition is mediated through the subversion of two key  
33 elements of innate immune surveillance. In the first, the role of TNF $\alpha$  changes from an  
34 antitumor effector against primary tumors into a growth promoter for MRD. Second, whereas  
35 primary tumors induced a natural killer (NK)-mediated cytokine response characterized by low  
36 IL6 and elevated IFN $\gamma$ , PD-L1<sup>hi</sup> MRD cells promoted the secretion of elevated levels of IL6 but  
37 minimal IFN $\gamma$ , inhibiting both NK cell and T-cell surveillance. Tumor recurrence was promoted  
38 by trauma- or infection-like stimuli inducing VEGF and TNF $\alpha$ , which stimulated the growth of  
39 MRD tumors. Finally, therapies which blocked PD1, TNF $\alpha$ , or NK cells delayed or prevented  
40 recurrence. These data show how innate immune surveillance mechanisms, which control  
41 infection and growth of primary tumors, are exploited by recurrent, competent tumors and  
42 identifies therapeutic targets in patients with MRD known to be at high risk of relapse.

43

44 **Introduction**

45 Tumor dormancy followed by potentially fatal, aggressive recurrence represents a major  
46 clinical challenge for successful treatment of malignant disease since recurrence occurs at times  
47 that cannot be predicted (1),(2-6). Tumor dormancy is the time following frontline treatment in  
48 which a patient is apparently free of detectable tumor, but after which, local or metastatic  
49 recurrence becomes clinically apparent(2-8). Dormancy results from the balance of tumor-cell  
50 proliferation and death through apoptosis, lack of vascularization, immune surveillance(2-5, 9-  
51 13), and cancer-cell dormancy and growth arrest(2-4). Dormancy is characterized by presence of  
52 residual tumor cells (minimal residual disease [MRD])(14) and can last for decades (2, 5, 15-17).

53 Recurrences are often phenotypically very different from primary tumors, representing  
54 the end product of *in vivo* selection against continued sensitivity to frontline treatment(18-28).  
55 Escape from frontline therapy is common, in part, because of the heterogeneity of tumor  
56 populations(29, 30), which include treatment-resistant subpopulations(31). Understanding the  
57 ways in which recurrent tumors differ from primary tumors would allow early initiation of  
58 rational, targeted second-line therapy. Identifying triggers which convert MRD into actively  
59 proliferating recurrence would allow more timely screening and early intervention to treat  
60 secondary disease(32).

61 To address these issues, we developed several different preclinical models in which  
62 suboptimal frontline treatment induced complete macroscopic regression, a period of dormancy  
63 or MRD, followed by local recurrence. Thus, treatment of either subcutaneous B16 melanoma  
64 or TC2 prostate tumors with adoptive T-cell transfer(21, 33-35), systemic virotherapy(36, 37),  
65 VSV-cDNA immunotherapy(38, 39), or ganciclovir (GCV) chemotherapy(40-42) led to  
66 apparent tumor clearance (no palpable tumor) for >40-150 days. However, with prolonged

67 follow-up, a proportion of these animals developed late, aggressive local recurrences, mimicking  
68 the clinical situation in multiple tumor types(43-45). Recurrence was associated with elevated  
69 expression of several recurrence-specific antigens that were shared across tumor types, such as  
70 YB-1 and Topoisomerase-II $\alpha$  (TOPO-II $\alpha$ ) (44), as well as tumor type-specific recurrence  
71 antigens(45).

72 Here, we show that the transition from MRD into actively proliferating recurrent tumors  
73 is mediated through the subversion of two key elements of innate immune surveillance of tumors  
74 – recognition by natural killer (NK) cells and response to TNF $\alpha$ . These data show how the  
75 transition from MRD to active recurrence is triggered *in vivo* and how recurrences use innate,  
76 antitumor immune effector mechanisms to drive their own expansion and escape from immune  
77 surveillance. Understanding these mechanisms can potentially lead to better treatments that delay  
78 or prevent tumor recurrence.

79

## 80 **Materials and Methods**

### 81 *Mice, cell lines, and viruses*

82 6-8 week old female C57Bl/6 mice were purchased from Jackson Laboratories (Bar  
83 Harbor, Maine). The OT-I mouse strain (on a C57BL/6 [H2-K<sup>b</sup>] background) was bred at the  
84 Mayo Clinic and expresses the transgenic T-cell receptor V $\alpha$ 2/V $\beta$ 5 specific for the SIINFEKL  
85 peptide of ovalbumin in the context of MHC class I, H-2K<sup>b</sup> as previously described(46). Pmel-1  
86 transgenic mice (on a C57BL/6 background) express the V $\alpha$ 1/V $\beta$ 13 T-cell receptor that  
87 recognizes amino acids 25-33 of gp100 of pmel-17 presented by H2-D<sup>b</sup> MHC class I  
88 molecules(47). Pmel-1 breeding colonies were purchased from The Jackson Laboratory at 6-8

89 weeks of age and were subsequently bred at Mayo Clinic under normal housing (not pathogen-  
90 free) conditions.

91 The B16ova cell line was derived from a B16.F1 clone transfected with a pcDNA3.1ova  
92 plasmid(33). B16ova cells were grown in DMEM (HyClone, Logan, UT, USA) containing 10%  
93 FBS (Life Technologies) and G418 (5 mg/mL; Mediatech, Manassas, VA, USA) until challenge.  
94 B16tk cells were derived from a B16.F1 clone transfected with a plasmid expressing the Herpes  
95 Simplex Virus thymidine kinase (HSVtk) gene. Following stable selection in puromycin (1.25  
96  $\mu\text{g}/\text{mL}$ ), these cells were shown to be sensitive to ganciclovir (GCV; cymevene) at 5  $\mu\text{g}/\text{ml}$ (40,  
97 41). For experiments where cells were harvested from mice, tumor lines were grown in DMEM  
98 containing 10% FBS and 1% Pen/Strep (Mediatech). Where appropriate, adherent cells were  
99 confirmed to be B16tk cells by the expression of melanin and by qrtPCR for the HSVtk gene.

100 Cells were authenticated by morphology, growth characteristics, PCR for melanoma  
101 specific gene expression (gp100, TYRP-1 and TYRP2) and biologic behavior, tested  
102 mycoplasma-free and frozen. Cells were cultured less than three months after resuscitation.

103 Wildtype Reovirus type 3 (Dearing strain) stock titers were measured by plaque assays  
104 on L929 cells (a kind gift from Dr. Kevin Harrington, Institute of Cancer Research, Fulham  
105 Road, London). Briefly, 6 well plates were seeded with 750,000 L929 cells/well in DEMEM +  
106 10%FBS and incubated overnight. Cells were washed once with PBS. 1ml of serial dilutions of  
107 the test Reovirus stocks were pipetted into each well, with each dilution run in duplicate. Cells  
108 were incubated with virus for 3 hours. Media and virus was aspirated off the cells and 2ml of  
109 1% Noble agar (diluted from a 2% stock with 2x DMEM/10% FBS) at 42°C was added to each  
110 well. Plates were incubated for 4-5 days until plaques were visible, when wells were stained  
111 with 500 $\mu\text{l}$  of 0.02% neutral red for 2 hours and plaques were counted.. For *in vivo* studies,

112 reovirus was administered intravenously (i.v.) at  $2 \times 10^7$  TCID<sub>50</sub> (50% tissue culture infective  
113 dose) per injection.

114 *In vivo experiments*

115 C57BL/6J (catalog no. 000664) and B6.129S2-*Il6*<sup>tm1Kopf</sup>/J IL-6 Knockout  
116 (catalog no. 002650) mice were purchased from the Jackson Laboratory.

117 All *in vivo* studies were approved by the Mayo IACUC. Mice were challenged  
118 subcutaneously (s.c) with  $5 \times 10^5$  B16ova, B16tk, or B16 melanoma cells in 100  $\mu$ L PBS  
119 (HyClone). Tumors were measured 3 times per week using Bel-Art SP Scienceware Dial-type  
120 calipers, and mice were euthanized with CO<sub>2</sub> when tumors reached 1.0 cm diameter.

121 For suboptimal adoptive T-cell therapy (in which more than 50% of treated mice would  
122 undergo complete macroscopic regression followed by local recurrence), mice were treated i.v.  
123 with PBS or  $10^6$  4-day activated OT-I T cells on days 6 and 7 post B16ova injection as  
124 previously described (21, 43).

125 For GCV chemotherapy experiments, C57BL/6 mice were treated with GCV  
126 intraperitoneally (i.p). at 50 mg/ml on days 6-10 and days 13-17 post s.c. B16tk injection.

127 For suboptimal, systemic virotherapy experiments, C57BL/6 mice with 5-day established  
128 B16 tumors were treated i.p. with PBS or paclitaxel (PAC) at 10 mg/kg body weight (Mayo  
129 Clinic Pharmacy, Rochester, MN) for 3 days followed by i.v. reovirus ( $2 \times 10^7$  TCID<sub>50</sub>) or PBS  
130 for 2 days. This cycle was repeated once and was modified from a more effective therapy  
131 previously described(36).

132 To prevent or delay tumor recurrences, mice were treated i.v. with anti-PD1 (0.25 mg;  
133 catalog no. BE0146; BioXcell, West Lebanon, NH), anti-TNF $\alpha$  (1  $\mu$ g; catalog no. AF-410-NA;  
134 R&D Systems), anti-asialo GM1 (0.1 mg; catalog no. CL8955; Cedarlane, Ontario, Canada) or

135 isotype control rat IgG (catalog no. 012-000-003; Jackson Immuno Research) antibody at times  
136 as described in each experiment.

#### 137 *Establishment of MRD tumor-cell cultures from skin explants*

138 Mice treated with GCV, OT-I T cells, or reovirus that had no palpable tumors following  
139 regression and macroscopic disappearance for >40 days had skin from the sites of B16tk,  
140 B16ova, or B16 injection explanted. Briefly, skin was mechanically and enzymatically  
141 dissociated and  $\sim 10^3$ - $10^4$  cells were plated in 24-well plates in DMEM containing 10% FBS and  
142 1% Pen/Strep. 24hrs later wells were washed three times with PBS, and 7 days later inspected  
143 microscopically for actively growing tumor-cell cultures.

#### 144 *Quantitative RT-PCR (qRT-PCR)*

145 B16 cells or MRD B16 cells expanded from a site of tumor injection for 72 hrs in TNF- $\alpha$   
146 *in vitro*, were cultured for 48 hours in serum-free medium. Cells were then harvested, and RNA  
147 was prepared with the QIAGEN RNeasy Mini Kit. 1  $\mu$ g total RNA was reverse-transcribed in a  
148 20  $\mu$ l volume using oligo-(dT) primers and the Transcriptor First Strand cDNA synthesis kit  
149 (catalog no. 04379012001; Roche). A LightCycler 480 SYBR Green I Master kit was used to  
150 prepare samples according to the manufacturer's instructions. Briefly, 1 ng of cDNA was diluted  
151 (neat [undiluted], 1:10, 1:100, 1:1000) and amplified with gene-specific primers using GAPDH  
152 as a normalization control. Expression of the murine TOPO-II $\alpha$  gene was detected using the  
153 forward 5'-GAGCCAAAATGTCTTGTATTAG-3' and reverse 5'-  
154 GAGATGTCTGCCCTTAGAAG-3' primers. Expression of the murine GAPDH gene was  
155 detected using the forward 5'-TCATGACCACAGTCCATGCC-3', and reverse 5'-  
156 TCAGCTCTGGGATGACCTTG-3' primers. Primers were designed using the NCBI Primer  
157 Blast primer designing tool.

158 Samples were loaded into a 96-well PCR plate in duplicate and ran on a LightCycler480  
159 instrument (Roche). The threshold cycle (Ct) at which amplification of the target sequence was  
160 detected was used to compare the relative expression of mRNAs in the samples using the  $2^{-\Delta\Delta Ct}$   
161 method.

#### 162 *Immune-cell activation*

163 Spleens and lymph nodes (LNs) were immediately excised from euthanized C57BL/6 or  
164 OT-I mice and dissociated *in vitro* to achieve single-cell suspensions. Red blood cells were lysed  
165 with ACK lysis buffer (Sigma-Aldrich, St. Louis, MO) for 2 minutes. Cells were resuspended at  
166  $1 \times 10^6$  cells/mL in Iscove's Modified Dulbecco's Medium (IMDM; Gibco, Grand Island, NY)  
167 supplemented with 5% FBS, 1% Pen-Strep, 40  $\mu$ M 2-BME. Cells were cocultured with target  
168 B16 or B16MRD cells as described in the text. Cell-free supernatants were then collected 72  
169 hours later and tested for IFN $\gamma$  (Mouse IFN $\gamma$  ELISA Kit; OptEIA, BD Biosciences, San Diego,  
170 CA) and TNF $\alpha$  (BD Biosciences, San Jose, CA) production by ELISA as directed in the  
171 manufacturer's instructions.

172 NK cells were prepared from spleens of naïve C57BL/6 mice using the NK Cell Isolation  
173 Kit II (Miltenyi, Auburn, CA) as described in the "NK cell isolation" section and cocultured with  
174 B16 or B16MRD target tumor cells at E:T ratios of 20:1. 72 hours later, supernatants were  
175 assayed for IFN $\gamma$  or IL6 by ELISA.

#### 176 *Cytokines and antibodies*

177 Cytokines and cytokine neutralizing antibodies were added to cultures upon plating of the  
178 cells and used at the following concentrations *in vitro*: VEGF<sub>165</sub> (12 ng/mL; catalog no. CYF-  
179 336; Prospec-Bio), TNF $\alpha$  (100 ng/mL; catalog no. 31501A; Peprotech), IL6 (100 pg/mL; catalog  
180 no. 216-16; PeproTech), anti-TNF $\alpha$  (0.4 $\mu$ g/ml; catalog no. AF410NA; R&D Systems), universal

181 IFN $\alpha$  (100U; catalog no. 11200-2; R&D Systems), anti-IL6 (1  $\mu$ g/ml; catalog no. MP5-20F3;  
182 BioLegend, San Diego), LPS (25 ng/ml; catalog no. L4524; Sigma), CpG (25 ng/ml; Mayo  
183 Clinic Oligonucleotide Core facility).

#### 184 *Immune cell depletion*

185 Splenocyte/LN cultures were depleted of different immune cell types (asialo GM-1<sup>+</sup>  
186 (NKs), CD4<sup>+</sup>, CD8<sup>+</sup>, CD11c<sup>+</sup>, or CD11b<sup>+</sup> cells) by magnetic bead depletion (catalog no. 130-  
187 052-501 (NK); 130-104-454 (CD4); 130-104-075 (CD8); 130-108-338 (CD11c) and 130-049-  
188 601 (CD11b), Miltenyi Biotec, CA, USA) according to the manufacturer's instructions.

189 In addition, splenocyte/LN cultures were depleted using the RB6-8C5 (8 $\mu$ g/ml) (R&D Systems,  
190 catalog no. MAB1037) and 1A8 (1 $\mu$ g/ml) (BioLegend, catalog no. 127601) antibodies. While  
191 1A8 recognizes only Ly-6G (Gr1), clone RB6-8C5 recognizes both Ly-6G and Ly-6C. Ly6G is  
192 differentially expressed in the myeloid lineage on monocytes, macrophages, granulocytes, and  
193 peripheral neutrophils. RB6-8C5 is typically used for phenotypic analysis of monocytes,  
194 macrophages and granulocytes whilst 1A8 is typically used to characterize neutrophils.

#### 195 *NK cell isolation and flow cytometry*

196 Mouse NK cells were isolated from single cell suspensions of the dissociated spleens of  
197 6-8 week old C57BL/6 mice using the NK Cell Isolation Kit II according to the manufacturer's  
198 instructions (Miltenyi Biotec, Auburn, CA). In this protocol, T cells, dendritic cells, B cells,  
199 granulocytes, macrophages, and erythroid cells are indirectly magnetically labeled with a  
200 cocktail of biotin-conjugated antibodies and anti-biotin microbeads for 15 minutes. After  
201 depleting magnetically labeled cells, isolation and enrichment of unlabeled NK cells was  
202 confirmed by flow cytometry. Isolated NK cells were stained with CD3-FITC (catalog no.  
203 100306; Biolegend, San Diego, CA), NK1.1-PE (catalog no. 108708; Biolegend), PD1-Pe/Cy7

204 (catalog no. 109109; Biolegend), PD-L1-APC (catalog no. 124311; Biolegend) to distinguish  
205 enriched NK cells from CD3<sup>+</sup> cells. Blood was taken either serially in a ~200 $\mu$ L submandibular  
206 vein bleed or from cardiac puncture at the time of sacrifice. Blood was collected in heparinized  
207 tubes, washed twice with ACK lysis buffer, and resuspended in PBS for staining.

208 Flow cytometry analysis was carried out by the Mayo Microscopy and Cell Analysis core  
209 and data were analyzed using FlowJo software (TreeStar, USA). Enriched NK cells were  
210 identified by gating on NK1.1<sup>hi</sup> CD49b<sup>hi</sup> CD3 $\epsilon$ <sup>lo</sup> cells.

#### 211 *In vitro cytokine secretion and flow cytometry*

212 B16 or B16MRD tumor cells cocultured with isolated NK cells were seeded in DMEM  
213 containing 10% FBS and 1% Pen/Strep containing anti-PD1 (catalog no. BE0146; Bio-X-cell,  
214 West Lebanon, NH), anti-PD-L1 (catalog no. BE0101; Bio-X-cell), anti-CTLA4 (100 ng/mL;  
215 catalog no. BE0164; Bio X Cell), or isotype control (Chrome Pure anti-Rabbit IgG; catalog no.  
216 011-000-003; Jackson Laboratories, Farmington, CT). 72 hours post-incubation, supernatants  
217 were harvested and analyzed for cytokine secretion using ELISAs for IFN $\gamma$  and TFN $\alpha$ . Tumor  
218 cells were stained for CD45-PerCP (BD Bioscience San Diego,CA) and PD-L1-APC (Biolegend,  
219 San Diego,CA). Flow cytometry analysis was performed as discussed.

#### 220 *Phase contrast microscopy*

221 Pictures of B16 or B16MRD cell cultures, under the conditions described in the text,  
222 were acquired using an Olympus-IX70 microscope (UplanF1 4x/0.13PhL), a SPOT Insight-1810  
223 digital camera and SPOT Software v4.6.

#### 224 *Histopathology*

225 Skin at the site of initial tumor cell injection or tumors was harvested, fixed in 10%  
226 formalin, paraffin-embedded, and sectioned. Two independent pathologists, blinded to the

227 experimental design, examined H&E sections for the presence of B16 melanoma cells and any  
228 immune infiltrate.

## 229 *Statistics*

230 *In vivo* experimental data were analyzed using GraphPad Prism 4 software (GraphPad  
231 Software, La Jolla, CA, USA). Survival data from the animal studies were analyzed using the  
232 log-rank test and the Mann-Whitney *U* test, and data were assessed using Kaplan-Meier plots.  
233 One-way ANOVA and two-way ANOVAs were applied for *in vitro* assays as appropriate.  
234 Statistical significance was determined at the level of  $p < 0.05$ .

235

## 236 **Results**

### 237 *Model of minimal residual disease (MRD)*

238 We have previously shown that established subcutaneous B16 tumors can be treated with  
239 either prodrug chemotherapy, oncolytic viro-immunotherapy, or adoptive T-cell therapy(21, 34,  
240 36, 43-45). Irrespective of the frontline treatment, histology at the site of initial tumor injection  
241 after tumor regression often showed residual melanoma cells in mice scored as tumor-free (Fig.  
242 1A).

243 In one experiment, 6/10 mice cleared of B16tk tumors by treatment with ganciclovir  
244 (using a regimen in which 100% of tumors regressed macroscopically followed by ~50-80% of  
245 the mice undergoing later local recurrence)(43) had histological evidence of MRD at 80d post  
246 tumor seeding. Although parental B16tk cells grow rapidly in tissue culture, no viable B16tk  
247 cells were recovered from separate skin explants 75d following tumor seeding from 15 mice  
248 which had undergone complete macroscopic regressions following ganciclovir (Fig. 1B and H).  
249 The very low frequency of regrowth of B16 cultures from skin explants was reproducible from

250 mice in which primary B16tk or B16ova tumors were rendered nonpalpable by oncolytic  
251 virotherapy with either reovirus(36), adoptive T-cell therapy with Pmel(34), or OT-I T cells(21)  
252 (see Table 1 for cumulative summary).

253         When C57BL/6 splenocytes from tumor-naive mice were cocultured with skin explants  
254 containing MRD B16 cells, no tumor cells were recovered after *in vitro* culture (Fig. 1C and H).  
255 However, when splenocyte and LN cells from mice which had previously cleared B16 tumors  
256 were cocultured with skin explants, actively proliferating B16 cultures could be recovered *in*  
257 *vitro* (Fig. 1D and H). These data suggest that splenocyte and LN cells from mice previously  
258 vaccinated against primary tumor cells, secret a factor which promotes growth of MRD B16  
259 cells. In this respect, systemic VEGF can prematurely induce early recurrence of B16 MRD  
260 following frontline therapy that cleared the tumors(43). Although *in vitro* treatment of MRD  
261 B16 explants with VEGF did not support outgrowth of B16 cells (Fig. 1E and H), coculture of  
262 splenocytes and LNs from control nontumor-bearing mice with VEGF supported outgrowth at  
263 low frequencies (Fig. 1F and H). However, coculture of splenocytes and LNs from mice that  
264 cleared B16 primary tumors with VEGF consistently supported outgrowth of MRD B16 cells  
265 with high efficiency (Fig. 1G).

#### 266 ***TNF $\alpha$ supports outgrowth of MRD***

267         VEGF-treated splenocyte and LN cells from mice that cleared B16 tumors showed rapid  
268 upregulation of TNF $\alpha$ , derived principally from CD11b<sup>+</sup> cells (Fig. 2A). Depletion of CD4<sup>+</sup> T  
269 cells enhanced TNF $\alpha$  production from VEGF-treated splenocyte and LN cells (Fig. 2A).  
270 Outgrowth of MRD B16 cells from skin explants following different frontline therapies was  
271 actively promoted by TNF $\alpha$  (Fig. 2B and F) but not by IL6 (Fig. 2C and F) or other cytokines  
272 such as IFN $\gamma$  (Fig. 2B-F). Antibody-mediated blockade of TNF $\alpha$  significantly inhibited the

273 ability of splenocyte and LN cells from mice that cleared B16 tumors to support outgrowth of  
274 MRD B16 cells (Fig. 2D-F). In contrast to the growth-promoting effects of TNF $\alpha$  on MRD B16  
275 cells, culture of parental B16 cells with TNF $\alpha$  significantly inhibited growth (Fig. 2G).  
276 Consistent with Fig. 2A, monocytes and macrophages were the principal source of the growth-  
277 promoting TNF $\alpha$  in VEGF-treated splenocyte and LN cells from mice that cleared B16 tumors  
278 (Fig. 2G). Similarly, outgrowth of MRD TC2 murine prostate cells following frontline viro-  
279 immunotherapy was also actively promoted by TNF $\alpha$ , whereas TNF $\alpha$  was highly cytotoxic to  
280 the parental tumor cells (Fig. 2I). Therefore, in two different cell types, TNF $\alpha$  changes from an  
281 antitumor effector against primary tumors into a growth promoter for MRD. B16 MRD cultures  
282 maintained in TNF $\alpha$  for up to six weeks retained their dependence upon the cytokine for  
283 continued *in vitro* proliferation. Withdrawal of TNF $\alpha$  did not induce cell death but prevented  
284 continued proliferation. Finally, we did not observe reversion to a phenotype in which TNF $\alpha$   
285 was growth inhibitory within a six-week period.

286 We did not observe any reduction in the ability of cultures to support outgrowth of MRD  
287 cells when depleted of neutrophils, CD4 cells, or NK cells, whereas depletion of Ly6G<sup>+</sup> cells  
288 (completely) and CD8<sup>+</sup> T cells (partially) inhibited outgrowth (Fig. 2H). Therefore, taken  
289 together with the dependence of TNF $\alpha$  production on CD11b<sup>+</sup> cells, our data suggest that  
290 CD11b<sup>+</sup> monocytes and macrophages are the principal cell type responsible for the TNF $\alpha$ -  
291 mediated outgrowth of B16 MRD recurrences, although CD8<sup>+</sup> T cells also play a role.

### 292 ***TNF $\alpha$ -expanded MRD acquires a recurrence competent phenotype***

293 The recurrence competent phenotype (RCP) of B16 cells emerging from a state of MRD  
294 is associated with transient high expression of Topoisomerase II $\alpha$  (TOPO-II $\alpha$ ) and YB-1(44) and  
295 acquired insensitivity to innate immune surveillance(43). Therefore, we investigated whether the

296 B16 MRD cultures, which we could induce with TNF $\alpha$ , resembled this same phenotype to  
297 validate their identity as recurrent tumors. MRD B16 cells expanded *in vitro* with TNF $\alpha$   
298 overexpressed both Topo-II $\alpha$  and YB-1 compared to parental B16, consistent with their  
299 acquisition of the RCP (Fig. 3A). Coculture of skin explants with TNF $\alpha$  or splenocyte and LN  
300 cultures induced outgrowth of MRD B16 cells (Fig. 3B and D), which were sensitive to the  
301 Topo-II $\alpha$ -targeting drug doxorubicin (Fig. 3C and E). MRD B16 cells expanded in TNF $\alpha$  were  
302 also insensitive to the antiviral protective effects of IFN $\alpha$  upon infection with reovirus and  
303 supported more vigorous replication of reovirus than parental B16 cells (Fig. 3F), consistent with  
304 acquisition of the RCP(43). In contrast, IFN $\alpha$  protected parental B16 cells from virus  
305 replication.

#### 306 ***MRD cells lose sensitivity to NK immune surveillance***

307 The recurrence competent phenotype is also associated with an acquisition of an  
308 insensitivity to innate immune effectors(44). Therefore, we next investigated whether NK cells,  
309 a major effector of innate immune surveillance of tumors, differentially recognized primary B16  
310 compared to their B16 MRD derivatives. For the following experiments, a homogenous  
311 population of untouched splenic NK1.1<sup>hi</sup> CD49b<sup>hi</sup> CD3 $\epsilon$ <sup>Lo</sup> NK cells were isolated from spleens  
312 of C57BL/6 mice. Although purified NK cells secreted significant amounts of IFN $\gamma$  upon  
313 coculture with parental B16 cells, TNF $\alpha$ -expanded MRD B16 cultures did not stimulate IFN $\gamma$   
314 from NK cells (Fig. 4A). Consistent with reports of a spike in serum IL6 just prior to the  
315 emergence of tumor recurrences(43), cocultures of purified NK cells from wildtype mice, but not  
316 from IL6 knockout mice, produced IL6 in response to MRD B16, but not parental B16, cells  
317 (Fig. 4B). Intracellular staining confirmed that an NK1.1<sup>+</sup> cell population within wildtype  
318 splenocytes differentially recognized parental B16 and B16 MRD cells through IL6 expression

319 (Fig. 4C). IL6 was detected in excised small recurrent tumors but not in small primary tumors,  
320 whereas TNF $\alpha$  could not be detected in recurrent tumors but was present at very low amounts in  
321 some primary tumors (Fig. 4D). Although subcutaneous injection of 10<sup>3</sup> MRD B16 cells  
322 generated tumors in 100% of mice, a similar dose of parental B16 cells did not generate tumors  
323 in any of the 5 animals (Figs. 4E and F). However, when mice were depleted of NK cells prior  
324 to tumor challenge, 10<sup>3</sup> parental B16 cells became tumorigenic in 100% of the animals (Fig.  
325 4E). NK cell depletion had no effect on the already high tumorigenicity of the same dose of  
326 MRD B16 cells (Fig. 4F). Therefore, MRD B16 cells expanded in TNF $\alpha$  were significantly more  
327 tumorigenic than parental B16 cells, in part, because they were insensitive to NK cell  
328 recognition.

#### 329 *Differential recognition of primary and MRD cells by NK cells*

330 Both MRD B16 cells expanded in TNF $\alpha$  and a freshly resected tumor upregulated the T-  
331 cell checkpoint inhibitory molecule PD-L1(48, 49), whereas PD-L1 expression was low on  
332 parental B16 cells and lower on a freshly resected primary tumor, whether or not it was treated  
333 with TNF $\alpha$  (Fig. 5A).

334 Although purified NK cells did not secrete IFN $\gamma$  in response to TNF $\alpha$ -expanded MRD B16 cells  
335 or to early recurrent B16 tumor explants (Fig. 4A), they did produce IFN $\gamma$  in the presence of  
336 parental B16 cells and primary B16 tumors (Fig. 5B). Blockade of PD-L1 on MRD B16 cells  
337 increased NK cell-mediated IFN $\gamma$  secretion and also significantly enhanced NK cell response to  
338 parental B16 cells (Fig. 5B). Conversely, NK cell-mediated IL6 secretion in response to MRD  
339 B16 cells was significantly decreased by blockade of PD-L1 (Fig. 5C). However, PD-L1  
340 blockade did not alter the inability of parental B16 cells to stimulate IL6 secretion from purified  
341 NK cells (Fig. 5C).

342 ***NK cell-mediated IL6 inhibits T-cell recognition of MRD***

343 MRD B16ova cells recovered from skin explants of B16ova primary tumors rendered to a  
344 state of MRD by adoptive OT-I T-cell therapy(21) still retained high expression of the target  
345 OVA antigen, suggesting that antigen loss is a later event in the progression to recurrent tumor  
346 growth (Fig. 5D). As expected, OT-I T cells secreted IFN $\gamma$  upon coculture with B16ova cells *in*  
347 *vitro* and was augmented by coculture with NK cells from either wildtype or IL6 KO mice (Fig.  
348 5E). Anti-IL6 had no effect on OT-I recognition of parental B16ova cells irrespective of the  
349 source of the NK cells (Fig. 5E). Although TNF $\alpha$ -expanded MRD B16ova cells still expressed  
350 OVA (Fig. 5D), they elicited significantly lower IFN $\gamma$  from OT-I and NK cells alone (Fig. 5F).  
351 Coculture of OT-I T cells with wildtype, but not with IL6 KO, NK cells abolished IFN $\gamma$   
352 production in response to MRD B16ova cells (Fig. 5F and G) and was reversed by IL6 blockade  
353 (Fig. 5F). After 7d of coculture with OT-I and NK cells, surviving parental B16ova cells had  
354 lost OVA expression, irrespective of the IL6 presence (Fig. 5H). However, only in the presence  
355 of IL6 blockade did MRD B16ova cells rapidly lose OVA expression (Fig.5G). These data  
356 suggest that NK-mediated IL6 expression in response to TNF $\alpha$ -expanded MRD cells can inhibit  
357 T-cell recognition of its cognate antigen expressed by tumor targets and, thereby, slow the  
358 evolution of antigen loss variants.

359 Phenotypic analysis of the lymphoid cells from tumor naive mice compared with those  
360 from mice cleared of tumor showed minimal differences in subsets of CD4<sup>+</sup> T cells (Fig. 6A-D).  
361 In addition to a non-significant trend towards an increase in circulating CD8<sup>+</sup> effector cells  
362 (CD44<sup>Hi</sup> CD62L<sup>Lo</sup>) in mice cleared of tumor (Fig. 6E), effector cells expressing both inhibitory  
363 receptors PD1 and TIM-3 were also consistently higher compared to tumor naïve mice (Fig. 6F).  
364 These data suggest that mice with tumors that have been treated successfully through

365 immunotherapeutic frontline treatments contain populations of antitumor effector cells that may  
366 be functionally impaired to some degree due to elevated expression of checkpoint inhibitor  
367 molecules.

### 368 ***Inhibition of tumor recurrence***

369         Based on these data, several molecules and cells – VEGF, CD11b<sup>+</sup> cells, TNF $\alpha$ , PD-L1,  
370 NK cells – would be predicted to play an important role in mediating the successful transition  
371 from MRD to actively expanding recurrence. After primary B16tk tumors had regressed  
372 following chemotherapy with GCV(43), about half of the mice routinely developed recurrences  
373 between 40-80 days following complete macroscopic regression of the primary tumor (Fig. 7A).  
374 However, long-term treatment with antibody-mediated blockade of either PD1 or TNF $\alpha$   
375 effectively slowed or prevented recurrence (Fig. 7A). The depletion of NK cells also prevented  
376 recurrence of B16tk tumors (Fig. 7A), consistent with their secretion of T-cell inhibitory IL6.

377         Our data would also predict that systemic triggers that induce VEGF(43) and/or TNF $\alpha$   
378 from host CD11b<sup>+</sup> cells would accelerate tumor recurrence. *In vitro*, LPS stimulation of  
379 splenocyte and LN cultures induced high TNF $\alpha$  (Fig. 7B) and also supported the outgrowth of  
380 5/8 MRD B16 skin explants, an effect which was eradicated by blockade of TNF $\alpha$  (Fig. 7C).  
381 Therefore, we tested systemic treatment with TNF $\alpha$ -inducing LPS as a mimic of a trauma or  
382 infection that may induce recurrence. Primary tumors that macroscopically regressed into a state  
383 of MRD were prematurely induced to recur in 100% of mice following treatment with LPS,  
384 consistent with an LPS/TNF $\alpha$  induced mechanism of induction of recurrence from a state of  
385 MRD (Fig. 7D). Under these conditions, depletion of NK cells significantly delayed recurrence  
386 but did not prevent it (Fig. 7D), unlike in the model of spontaneous recurrence (Fig. 7A).  
387 Prolonged treatment with antibody-mediated blockade of either PD1 or TNF $\alpha$  successfully

388 prevented long-term recurrence, even when mice were treated with LPS (in 100% of mice in the  
389 experiment of Fig. 7D, and in 7/8 mice in a second experiment).

390

## 391 **Discussion**

392 We have developed models in which several different frontline therapies reduced  
393 established primary tumors to a state of MRD with no remaining palpable tumor(43-45).  
394 However, in a proportion of mice in this study, frontline therapy was insufficient to eradicate all  
395 tumor cells, leaving histologically detectable disease. Explants of skin at the site of tumor cell  
396 injection following regression rarely yielded actively proliferating B16 cells, even though >50%  
397 of samples contained residual tumor cells. The frequency with which cultures of MRD cells  
398 were recovered following explant was significantly increased by coculture with splenocytes and  
399 LN cells from mice previously treated for tumors, and this effect was enhanced by VEGF , which  
400 induced TNF $\alpha$  from CD11b+ cells. Taken together, we believe that CD11b+ monocytes and  
401 macrophages are the principal cell type responsible for the VEGF-mediated induction of TNF $\alpha$   
402 and for the TNF $\alpha$ -mediated outgrowth of B16 MRD recurrences. Although we showed TNF $\alpha$   
403 was highly cytotoxic to parental B16 cells and primary tumor explants, TNF $\alpha$  supported  
404 expansion of MRD cells from skin explants at high frequency, irrespective of the primary  
405 treatment. As shown previously, splenocytes from mice with cleared B16 tumors after GCV  
406 treatment killed significantly higher numbers of target B16 cells *in vitro* than did splenocytes  
407 from control, tumor naïve mice, confirming the generation of an effective antitumor T-cell  
408 response(42). In contrast, here we show no significant difference between killing of B16MRD  
409 cells expanded for 120hrs in TNF $\alpha$  *in vitro* by splenocytes from mice that cleared a B16 tumor  
410 compared to splenocytes from control, tumor naive mice. We are currently investigating the

411 molecular mechanisms by which B16MRD cells effectively evade the antitumor T-cell responses  
412 induced by frontline treatment (such as GCV, T-cell therapy, or oncolytic virotherapy).

413       TNF $\alpha$ -mediated expansion of MRD B16 cells induced the recurrence competent  
414 phenotype (RCP)(43, 44), shown by *de novo* expression of recurrence-associated genes (YB-1  
415 and Topoisomerase II $\alpha$ )(44). Re-activation of metastatic cells lying latent in the lungs has been  
416 associated with expression of the Zeb1 transcription factor, which mediates the epithelial-to-  
417 mesenchymal transition (EMT)(50). NK cells are major innate effectors of immune surveillance  
418 of tumors and responded differently to recurrent competent MRD B16 cells compared to  
419 primary B16 cells. We show NK cells were activated by parental B16 cells to secrete IFN $\gamma$  and  
420 were major effectors of *in vivo* tumor clearance. In contrast, TNF $\alpha$ -expanded MRD B16 cells  
421 induced NK cells to secrete IL6 instead of IFN $\gamma$ , which was not seen for parental B16 cells,  
422 effects mediated, in part, through PD-L1. IL6 produced by NK cells in response to TNF $\alpha$ -  
423 expanded MRD B16ova cells also inhibited OT-I T-cell recognition of OVA<sup>+</sup> tumor targets.  
424 TNF $\alpha$ -expanded MRD cells still retained expression OVA, despite using frontline OVA-targeted  
425 T-cell therapy. Only upon prolonged coculture of OVA<sup>+</sup> MRD cells with OT-I<sup>+</sup> NK cells with  
426 IL6 blockade was significant antigen loss observed, consistent with the long-term, but not early,  
427 loss of OVA antigen expression from B16ova recurrences following OT-I adoptive T-cell  
428 therapy(43) (21). Therefore, antigen loss in MRD cells is not an essential prerequisite for the  
429 emergence of tumor recurrences (21) and may occur through powerful selective pressure on very  
430 early antigen positive recurrent tumors as they expand *in vivo* in the presence of ongoing antigen  
431 targeted T-cell pressure.

432       Our data here are consistent with a model in which the transition from quiescent MRD to  
433 actively expanding recurrence is promoted by the acquisition of a phenotype in which TNF $\alpha$

434 changes from being a cytotoxic growth inhibitor (against primary tumors), to promoting the  
435 survival and growth of one, or a few, MRD cells. It is not clear whether these TNF $\alpha$  responsive  
436 clones exist within the primary tumor population, perhaps as recurrence competent stem  
437 cells(31), or whether this RCP is acquired by ongoing mutation during the response to frontline  
438 therapy(9, 14, 29, 30). Since established primary B16 and B16 MRD tumors both have low  
439 intratumoral NK infiltration, we hypothesize that the differential recognition of B16 or B16  
440 MRD cells by NK cells occurs at very early stages of tumor development. Therefore, it may be  
441 that different subsets of NK cells mediate the differential recognition of primary B16 (rejection)  
442 or B16 MRD (growth stimulation). However, in our experiments here a homogenous population  
443 of untouched splenic NK1.1<sup>hi</sup> CD49b<sup>hi</sup> CD3 $\epsilon$ <sup>lo</sup> NK cells differentially recognized parental B16  
444 and B16 MRD cells, suggesting that the basis for these different NK responses are, in large part,  
445 due to tumor-cell intrinsic properties. These recurrence competent MRD cells are insensitive to  
446 both innate and adaptive immune surveillance mechanisms, in part, through expression of PD-  
447 L1. With respect to escape from adaptive immune surveillance, we show both that the MRD cells  
448 express high levels of PD-L1 and that the fraction of effector cells expressing both inhibitory  
449 receptors PD1 and TIM-3 was consistently higher in tumor experienced mice than tumor naïve  
450 mice. Integral to both innate and adaptive immune evasion, TNF $\alpha$ -expanded MRD tumor cells  
451 induced an anti-inflammatory profile of IL6<sup>hi</sup> and IFN $\gamma$ <sup>lo</sup> expression from NK cells, the opposite  
452 of the profile of NK recognition (IL6<sup>lo</sup> IFN $\gamma$ <sup>hi</sup>) induced by parental primary tumor cells. This  
453 altered role of NK cells as prorecurrence effectors, as opposed to antitumor immune effectors,  
454 was due to impaired killing of MRD cells and recurrent tumor cells plus the secretion of IL6.  
455 This NK-derived IL6, in turn, inhibited T-cell responses against recurrent tumors, even when  
456 they continued to express T cell-specific antigens.

457 This model showed several molecules and cells – VEGF, CD11b<sup>+</sup> cells, TNF $\alpha$ , PD1/PD-  
458 L1, NK cells –can be targeted for therapeutic intervention to delay recurrence. In our model of  
459 spontaneous recurrence, depletion of NK cells or antibody-mediated blockade of either TNF $\alpha$  or  
460 PD1, significantly inhibited tumor recurrence following frontline GCV. Our data suggests that a  
461 systemic trigger – such as VEGF-induced by trauma or infection – promotes TNF $\alpha$  release from  
462 host CD11b<sup>+</sup> cells leading to growth stimulation of MRD cells. Consistent with this, LPS both  
463 induced TNF $\alpha$  from splenocytes and LN cells and mimicked TNF $\alpha$  in the generation of  
464 expanding MRD cultures from skin explants. Recurrence could be induced prematurely by LPS,  
465 as a mimic of a systemic infection/trauma, consistent with a report in which LPS treatment re-  
466 activated intravenously injected disseminated tumor cells pre-selected for properties of  
467 latency(50). These results suggest that patients in a state of MRD may be at significantly  
468 increased risk of recurrence following infections and/or trauma, which induce the release of  
469 systemic VEGF and/or TNF $\alpha$ . However, blockade of PD1 or TNF $\alpha$  following this trauma-like  
470 event prevented tumor recurrence. We are currently investigating when, and for how long, these  
471 potentially expensive recurrence blocking therapies will be required to be administered in  
472 patients. This is especially relevant for those patients in whom MRD may be present over  
473 several years before recurrence is triggered. Transcriptome analysis of MRD and early  
474 recurrences, compared to parental tumor cells, is underway in both mouse models (B16 and TC2)  
475 as well as in patient samples where matched pairs of primary and treatment failed recurrence  
476 tumors are available. These studies will identify the signaling pathways which differ between  
477 the cell types to account for their differential responses to TNF $\alpha$  signaling and IFN $\gamma$  and IL6  
478 production by NK cells. Future studies will focus on identifying which cells become recurrent  
479 tumors, the mutational and selective processes involved in the transition, identification of the

480 biological triggers for recurrence(1, 32), and the time over which recurrence inhibiting therapies  
481 must be administered.

482           In summary, we show here that the transition from MRD to recurrence involves the  
483 subversion of normal innate immune surveillance mechanisms. In particular, TNF $\alpha$  produced in  
484 response to pathological stimuli becomes a prorecurrence, as opposed to antitumor, growth  
485 factor. Simultaneously, NK cells, which normally restrict primary tumor growth, fail to kill  
486 expanding recurrent tumor cells and produce IL6 that helps to suppress adaptive T-cell  
487 responses, even with continued expression of T cell–targetable antigens. Finally, our data show  
488 that therapies aimed at blocking certain key molecules (PD1, TNF $\alpha$ ) and cell types (NK cells)  
489 may be valuable in preventing this transition from occurring in patients.

490

491 **Acknowledgments**

492 The authors thank Toni L. Higgins for expert secretarial assistance.

493

494

495 **References**

- 496 1. Yeh AC,Ramaswamy S. Mechanisms of Cancer Cell Dormancy--Another Hallmark of  
497 Cancer? *Cancer Res* 2015;75:5014-22.
- 498 2. Aguirre-Ghiso JA. Models, mechanisms and clinical evidence for cancer dormancy. *Nat*  
499 *Rev Cancer* 2007;7:834-46.
- 500 3. Goss PE,Chambers AF. Does tumour dormancy offer a therapeutic target? *Nat Rev*  
501 *Cancer* 2010;10:871-77.
- 502 4. Hensel JA, Flaig TW,Theodorescu D. Clinical opportunities and challenges in targeting  
503 tumour dormancy. *Nat Rev Clin Oncol* 2013;10:41-51.
- 504 5. McGowan PM, Kirstein JM,Chambers AF. Micrometastatic disease and metastatic  
505 outgrowth: clinical issues and experimental approaches. *Future Oncol* 2009;5:1083-98.
- 506 6. Pantel K, Alix-Panabieres C,Riethdorf S. Cancer micrometastases. *Nat Rev Clin Oncol*  
507 2009;6:339-51.
- 508 7. Aguirre-Ghiso JA, Bragado P,Sosa MS. Metastasis awakening: targeting dormant cancer.  
509 *Nature Med* 2013;19:276-7.
- 510 8. Polzer B,Klein CA. Metastasis awakening: the challenges of targeting minimal residual  
511 cancer. *Nature Med* 2013;19:274-5.
- 512 9. Baxevanis CN,Perez SA. Cancer Dormancy: A Regulatory Role for Endogenous  
513 Immunity in Establishing and Maintaining the Tumor Dormant State. *Vaccines*  
514 2015;3:597-619.
- 515 10. Albini A, Tosetti F, Li VW, Noonan DM,Li WW. Cancer prevention by targeting  
516 angiogenesis. *Nat Rev Clin Oncol* 2012;9:498-509.

- 517 11. Almog N, Ma L, Raychowdhury R, Schwager C, Erber R, Short S, et al. Transcriptional  
518 switch of dormant tumors to fast-growing angiogenic phenotype. *Cancer Res*  
519 2009;69:836-44.
- 520 12. Indraccolo S, Stievano L, Minuzzo S, Tosello V, Esposito G, Piovan E, et al. Interruption  
521 of tumor dormancy by a transient angiogenic burst within the tumor microenvironment.  
522 *Proc Natl Acad Sci U S A* 2006;103:4216-21.
- 523 13. Murdoch C, Muthana M, Coffelt SB, Lewis CE. The role of myeloid cells in the  
524 promotion of tumour angiogenesis. *Nat Rev Cancer* 2008;8:618-31.
- 525 14. Blatter S, Rottenberg S. Minimal residual disease in cancer therapy--Small things make  
526 all the difference. *Drug Resist Updat* 2015;21-22:1-10.
- 527 15. Karrison TG, Ferguson DJ, Meier P. Dormancy of mammary carcinoma after  
528 mastectomy. *J Natl Cancer Inst* 1999;91:80-5.
- 529 16. Kovacs AF, Ghahremani MT, Stefenelli U, Bitter K. Postoperative chemotherapy with  
530 cisplatin and 5-fluorouracil in cancer of the oral cavity and the oropharynx--long-term  
531 results. *J Chemother* 2003;15:495-502.
- 532 17. Retsky MW, Demicheli R, Hrushesky WJ, Baum M, Gukas ID. Dormancy and surgery-  
533 driven escape from dormancy help explain some clinical features of breast cancer.  
534 *APMIS* 2008;116:730-41.
- 535 18. Drake CG, Jaffee EM, Pardoll DM. Mechanisms of immune evasion by tumors. *Adv.*  
536 *Immunol.* 2006;90:51-81.
- 537 19. Garrido F, Cabrera T, Aptsiauri N. "Hard" and "soft" lesions underlying the HLA class I  
538 alterations in cancer cells: implications for immunotherapy. *Int J Cancer* 2010;127:249-  
539 56.

- 540 20. Goldberger O, Volovitz I, Machlenkin A, Vadai E, Tzehoval E, Eisenbach L. Exuberated  
541 numbers of tumor-specific T cells result in tumor escape. *Cancer Res* 2008;68:3450-7.
- 542 21. Kaluza KM, Thompson J, Kottke T, Flynn Gilmer HF, Knutson D, Vile R. Adoptive T  
543 cell therapy promotes the emergence of genomically altered tumor escape variants. *Int J*  
544 *Cancer* 2012;131:844-54.
- 545 22. Liu K, Caldwell SA, Greenelch KM, Yang D, Abrams SI. CTL adoptive immunotherapy  
546 concurrently mediates tumor regression and tumor escape. *J Immunol* 2006;176:3374-82.
- 547 23. Liu VC, Wong LY, Jang T, Shah AH, Park I, Yang X, et al. Tumor evasion of the  
548 immune system by converting CD4+CD25- T cells into CD4+CD25+ T regulatory cells:  
549 role of tumor-derived TGF-beta. *J Immunol* 2007;178:2883-92.
- 550 24. Movahedi K, Guilliams M, Van den Bossche J, Van den Bergh R, Gysemans C, Beschin  
551 A, et al. Identification of discrete tumor-induced myeloid-derived suppressor cell  
552 subpopulations with distinct T cell-suppressive activity. *Blood* 2008;111:4233-44.
- 553 25. Nagaraj S, Gupta K, Pisarev V, Kinarsky L, Sherman S, Kang L, et al. Altered  
554 recognition of antigen is a mechanism of CD8+ T cell tolerance in cancer. *Nat Med*  
555 2007;13:828-35.
- 556 26. Sanchez-Perez L, Kottke T, Diaz RM, Thompson J, Holmen S, Daniels G, et al. Potent  
557 selection of antigen loss variants of B16 melanoma following inflammatory killing of  
558 melanocytes in vivo. *Can Res* 2005;65:2009-17.
- 559 27. Uyttenhove C, Maryanski J, Boon T. Escape of mouse mastocytoma P815 after nearly  
560 complete rejection is due to antigen-loss variants rather than immunosuppression. *J Exp*  
561 *Med* 1983;157:1040-52.

- 562 28. Yee C, Thompson JA, Byrd D, Riddell SR, Roche P, Celis E, et al. Adoptive T cell  
563 therapy using antigen-specific CD8+ T cell clones for the treatment of patients with  
564 metastatic melanoma: in vivo persistence, migration, and antitumor effect of transferred  
565 T cells. *Proc Natl Acad Sci U S A* 2002;99:16168-73.
- 566 29. Gerlinger M, Rowan AJ, Horswell S, Larkin J, Endesfelder D, Gronroos E, et al.  
567 Intratumor heterogeneity and branched evolution revealed by multiregion sequencing.  
568 *New Engl J Med* 2012;366:883-92.
- 569 30. Marusyk A, Almendro V, Polyak K. Intra-tumour heterogeneity: a looking glass for  
570 cancer? *Nature reviews. Cancer* 2012;12:323-34.
- 571 31. Lawson DA, Bhakta NR, Kessenbrock K, Prummel KD, Yu Y, Takai K, et al. Single-cell  
572 analysis reveals a stem-cell program in human metastatic breast cancer cells. *Nature*  
573 2015;526:131-5.
- 574 32. Giancotti FG. Mechanisms governing metastatic dormancy and reactivation. *Cell*  
575 2013;155:750-64.
- 576 33. Kaluza K, Kottke T, Diaz RM, Rommelfanger D, Thompson J, Vile RG. Adoptive  
577 transfer of cytotoxic T lymphocytes targeting two different antigens limits antigen loss  
578 and tumor escape. *Hum Gene Ther* 2012;23:1054-64.
- 579 34. Rommelfanger DM, Wongthida P, Diaz RM, Kaluza KM, Thompson JM, Kottke TJ, et  
580 al. Systemic combination virotherapy for melanoma with tumor antigen-expressing  
581 vesicular stomatitis virus and adoptive T-cell transfer. *Cancer Res* 2012;72:4753-64.
- 582 35. Wongthida P, Diaz RM, Pulido C, Rommelfanger D, Galivo F, Kaluza K, et al.  
583 Activating systemic T-cell immunity against self tumor antigens to support oncolytic  
584 virotherapy with vesicular stomatitis virus. *Human Gene Ther* 2011;22:1343-53.

- 585 36. Kottke T, Chester J, Ilett E, Thompson J, Diaz R, Coffey M, et al. Precise scheduling of  
586 chemotherapy primes VEGF-producing tumors for successful systemic oncolytic  
587 virotherapy. *Mol Ther* 2011;19:1802-12.
- 588 37. Kottke T, Hall G, Pulido J, Diaz RM, Thompson J, Chong H, et al. Antiangiogenic cancer  
589 therapy combined with oncolytic virotherapy leads to regression of established tumors in  
590 mice. *J Clin Invest* 2010;120:1551-60.
- 591 38. Kottke T, Errington F, Pulido J, Galivo F, Thompson J, Wongthida P, et al. Broad  
592 antigenic coverage induced by viral cDNA library-based vaccination cures established  
593 tumors. *Nature Med* 2011;2011:854-59.
- 594 39. Pulido J, Kottke T, Thompson J, Galivo F, Wongthida P, Diaz RM, et al. Using virally  
595 expressed melanoma cDNA libraries to identify tumor-associated antigens that cure  
596 melanoma. *Nat Biotechnol* 2012;30:337-43.
- 597 40. Melcher AA, Todryk S, Hardwick N, Ford M, Jacobson M, Vile RG. Tumor  
598 immunogenicity is determined by the mechanism of cell death via induction of heat  
599 shock protein expression. *Nat Med* 1998;4:581-87.
- 600 41. Sanchez-Perez L, Gough M, Qiao J, Thanarajasingam U, Kottke T, Ahmed A, et al.  
601 Synergy of adoptive T-cell therapy with intratumoral suicide gene therapy is mediated by  
602 host NK cells. *Gene Ther* 2007;14:998-1009.
- 603 42. Vile RG, Castleden SC, Marshall J, Camplejohn R, Upton C, Chong H. Generation of an  
604 anti-tumour immune response in a non-immunogenic tumour: HSVtk-killing in vivo  
605 stimulates a mononuclear cell infiltrate and a Th1-like profile of intratumoural cytokine  
606 expression. *Int J Cancer* 1997;71:267-74.

607 43. Kottke T, Boisgerault N, Diaz RM, Donnelly O, Rommelfanger-Konkol D, Pulido J, et  
608 al. Detecting and targeting tumor relapse by its resistance to innate effectors at early  
609 recurrence. *Nature Med* 2013;19:1625-31.

610 44. Boisgerault N, Kottke T, Pulido J, Thompson J, Diaz RM, Rommelfanger-Konkol D, et  
611 al. Functional cloning of recurrence-specific antigens identifies molecular targets to treat  
612 tumor relapse. *Mol Ther* 2013;21:1507-16.

613 45. Zaidi S, Blanchard M, Shim K, Ilett E, Rajani K, Parrish C, et al. Mutated BRAF  
614 emerges as a major effector of recurrence in a murine melanoma model after treatment  
615 with immunomodulatory agents. *Mol Ther* 2014;23:845-56.

616 46. Hogquist KA, Jameson SC, Heath WR, Howard JL, Bevan MJ, Carbone FR. T cell  
617 receptor antagonistic peptides induce positive selection. *Cell* 1994;76:17-27.

618 47. Overwijk W, Theoret M, Finkelstein S, Surman D, de Jong L, Vyth-Dreese F, et al.  
619 Tumor regression and autoimmunity after reversal of a functionally tolerant state of self-  
620 reactive CD8+ T cells. *J. Exp. Med.* 2003;198:569-80.

621 48. Francisco LM, Sage PT, Sharpe AH. The PD-1 pathway in tolerance and autoimmunity.  
622 *Immunological reviews* 2010;236:219-42.

623 49. Brahmer JR, Tykodi SS, Chow LQ, Hwu WJ, Topalian SL, Hwu P, et al. Safety and  
624 activity of anti-PD-L1 antibody in patients with advanced cancer. *New Engl J Med*  
625 2012;366:2455-65.

626 50. De Cock JM, Shibue T, Dongre A, Keckesova Z, Reinhardt F, Weinberg RA.  
627 Inflammation triggers Zeb1-dependent escape from tumor latency. *Cancer Res* 2016;DOI  
628 10.1158/0008-5472.CAN-16-0608:Epub ahead of print.

629

630 **Figure Legends**

631 **Figure 1. Model of minimal residual disease. A-G**, Histological sections; **A**, Skin at the site  
632 of B16 cell injection from a C57BL/6 mouse treated with Pmel adoptive T-cell therapy with  
633 VSV-gp100 viro-immunotherapy(34). **B-D**, Skin explants from the site of B16tk cell injection  
634 from mice treated with GCV (no palpable tumor after regression) were **B**, left untreated; **C**,  
635 cocultured with  $10^5$  splenocytes and LN cells from normal C57BL/6 mice; or **D**, cocultured with  
636  $10^5$  splenocytes and LN cells from C57BL/6 mice cleared of B16tk tumors after GCV treatment.  
637 7 days later, wells were inspected for actively growing tumor cells. Images are representative of  
638 nine independent experiments with explants from different primary treatments. **E-H**, Skin from  
639 the sites of cleared B16tk tumors were explanted and treated as in **B** and were cocultured with **E**,  
640 VEGF (12ng/ml); **F**, VEGF and  $10^5$  splenocytes and LN cells from normal C57BL/6 mice; or **G**,  
641 VEGF and  $10^5$  splenocytes and LN cells from C57BL/6 mice cleared of B16tk tumors after GCV  
642 treatment. 3 separate explants per treatment were counted. **H**, Quantitation of **B-G**.

643 **Figure 2. MRD cells use TNF $\alpha$  as a growth factor. A**,  $10^5$  splenocytes and LN cells from  
644 C57BL/6 mice cleared of B16tk tumors (after GCV) were depleted of asialo GM-1<sup>+</sup> (NKs),  
645 CD4<sup>+</sup>, CD8<sup>+</sup>, CD11c<sup>+</sup>, or CD11b<sup>+</sup> cells by magnetic bead depletion and plated in the presence or  
646 absence of VEGF<sub>165</sub> (12ng/ml) in triplicate. Cell supernatants were assayed for TNF $\alpha$  by ELISA  
647 after 48 hours. Mean and standard deviation of triplicate wells are shown. Representative of two  
648 separate experiments. \*\*\*  $p < 0.0001$  (t Test). **B and C**, Skin from the B16tk cell injection site  
649 from mice treated with GCV (no palpable tumor after regression) was treated with **B**, TNF $\alpha$   
650 (100ng/ml) or **C**, IL6 (100pg/ml). 7 days later, wells were inspected for actively growing tumor  
651 cell cultures. Images are representative of 15 skin explants over five different experiments. **D**  
652 **and E**, Skin explants from the site of B16tk cell injection of mice treated with GCV (no palpable

653 tumor)cocultured with  $10^5$  splenocytes and LN cells from C57BL/6 mice cleared of B16tk  
654 tumors after GCV treatment (**D**) alone; or (**E**) in the presence of anti-TNF $\alpha$  (0.4 $\mu$ g/ml) 7 days  
655 later, wells were inspected for actively growing tumor cells. Images are representative of 5  
656 separate explants. (**F**) Quantitation of **B-E**. 3 separate explants per treatment were counted. **G**,  
657  $10^4$  parental B16 cells, explanted B16 cells from a PBS-treated mouse, or cells from two MRD  
658 B16 cultures (expanded *in vitro* in TNF $\alpha$  for 72 hrs) were plated in triplicate and grown in the  
659 presence or absence of TNF $\alpha$  for 4 days. Surviving cells were counted. Mean and standard  
660 deviation of triplicates are shown. Representative of three experiments. \* $p$ <0.01; \*\*  $p$ <0.001  
661 (ANOVA). **H**, Splenocytes and LN cells from C57BL/6 mice cleared of B16tk tumors after  
662 GCV treatment were treated with no antibody or with depleting antibodies specific for CD8,  
663 CD4, asialo GM-1(NK cells), monocytes and macrophages, or neutrophils. Skin samples from  
664 regressed tumor sites were cocultured with  $10^5$  depleted or non-depleted splenocytes and LN  
665 cultures in the presence of VEGF<sub>165</sub> (12ng/ml). 7 days later, wells were inspected for actively  
666 growing tumor cell cultures. The percentage of cultures positive for active MRD growth (wells  
667 contained  $>10^4$  adherent B16 cells) is shown. **I**,  $10^4$  explanted TC2 tumor cells from a PBS-  
668 treated mouse or cells from two MRD TC2 cultures (expanded *in vitro* in TNF $\alpha$  for 72 hrs) were  
669 plated in triplicate and grown in the presence or absence of TNF $\alpha$  for 4 days. Surviving cells  
670 were counted. Mean and standard deviation of triplicates are shown. \* $p$ <0.01; \*\*  $p$ <0.001  
671 (ANOVA).

672

673 **Figure 3. TNF $\alpha$ -expanded MRD cells acquire the recurrence competent phenotype.** **A**, 5 x  
674  $10^4$  B16 cells or MRD B16 cells (expanded from a site of tumor injection for 72 hrs in TNF $\alpha$ )  
675 were plated in triplicate. 24 hours later, cDNA was analyzed by qrtPCR for expression of YB-1

676 or TOPO-II $\alpha$ . Relative quantities of mRNA were determined. \* $p$ <0.05; Mean of the triplicate is  
677 shown. Representative of two separate experiments with two different B16 MRD recurrences.  
678 **B-E**, Skin explant from the B16tk cell injection site from mice treated with GCV was plated with  
679 **B**, TNF $\alpha$  (100ng/ml); **C**, TNF $\alpha$  plus doxorubicin (0.1mg/ml); or cocultured with VEGF and 10<sup>5</sup>  
680 splenocytes and LN cells from C57BL/6 mice cleared of B16tk tumors after GCV treatment **D**,  
681 without; or **E**, with doxorubicin. 7 days later, wells were inspected for actively growing tumor  
682 cells. Representative of three B16 MRD explants. **F**, 10<sup>3</sup> B16 cells or MRD B16 cells  
683 (expanded from a site of tumor injection for 72 hrs in TNF $\alpha$ ) were plated in triplicate. Cells  
684 were infected with reovirus (MOI 1.0) in the presence or absence of IFN $\alpha$  (100U) for 48 hours  
685 and titers of reovirus determined. Mean and standard deviation of triplicates are shown, \*\*  
686  $p$ <0.001 (ANOVA).

687  
688 **Figure 4. Parental and MRD cells are differentially recognized by NK cells.** B16 or MRD  
689 B16 cells (10<sup>5</sup> per well) were cocultured in triplicate with purified NK cells from either wildtype  
690 C57BL/6 (IL6+) or IL6 KO mice at an effector:target ratio of 20:1. 72 hours later, supernatants  
691 were assayed for **A**, IFN $\gamma$ ; or **B**, IL6 by ELISA. Mean and standard deviation of triplicates are  
692 shown, \* $p$ <0.05 \*\*  $p$ <0.001 (ANOVA). Representative of three separate experiments. **C**,  
693 Splenocytes and LN cells from wildtype C57BL/6 mice were plated with B16 or B16 MRD #2  
694 cells and grown for 72hrs in TNF $\alpha$  at an effector:target ratio of 50:1. 72 hours later, cells were  
695 harvested and analyzed for expression of NK1.1 and IL6. **D**, Three small primary B16ova  
696 tumors (<0.3cm diameter, Pri#1-3) from PBS-treated C57BL/6 mice or three small recurrent  
697 B16ova tumors from mice were excised, dissociated, and plated in 24-well plates overnight  
698 then supernatants were assayed for IL6 and TNF $\alpha$  by ELISA. Mean and standard deviation of

699 triplicates are shown; \*\*\*  $p < 0.0001$ , for IL6 between primary and recurrent tumors (t test). **E**  
700 **and F**, C57BL/6 mice (n= 5 mice/group) were challenged subcutaneously with **E**, parental  
701 B16ova cells; or **F**, B16ova MRD cells (expanded from a regressed B16ova tumor site for 72 hrs  
702 in TNF $\alpha$ ) at doses of  $10^3$  or  $10^4$  cells per injection. Included in E and F is a group of mice  
703 depleted of NK cells using anti-asialo GM-1 and challenged with  $10^3$  B16 or B16 MRD cells.  
704 Representative of two separate experiments. Survival analysis was conducted using log-rank  
705 tests. The threshold for significance was determined by using the Bonferroni correction for  
706 multiple comparisons.

707 **Figure 5. PD-L1 expression on MRD inhibits immune surveillance through IL6. A,**  
708 Expression of PD-L1 was analyzed by flow cytometry on parental B16 cells in culture. Cells  
709 from a small (~0.3cm diameter) B16tk tumor explanted from a PBS-treated mouse were cultured  
710 for 72 hrs *in vitro* alone (B16-PBS#1; dark blue) or with TNF $\alpha$  (B16-PBS#1+TNF $\alpha$ ; green).  
711 B16 MRD cells recovered from the site of B16tk cell injection after regression were treated with  
712 TNF $\alpha$  for 72 hrs (B16 MRD + TNF $\alpha$  72 hrs; purple). Cells from a small recurrent B16tk tumor  
713 (~0.3cm diameter) explanted following regression after GCV treatment was cultured for 72  
714 hours without TNF $\alpha$  (B16 REC#1; light blue). Representative of three separate experiments. **B**  
715 **and C**, MRD B16 cells expanded for 72hrs in TNF $\alpha$ , parental B16 cells, explanted B16tk  
716 recurrent tumor cells, or explanted primary B16 tumors were plated ( $10^4$  cells per well). 24  
717 hours later,  $10^5$  purified NK cells from C57BL/6 mice were added to the wells with control IgG  
718 or anti-PD-L1. 48 hours later supernatants were assayed for **B**, IFN $\gamma$  or **C**, IL6 by ELISA. Mean  
719 of triplicates per treatment are shown. Representative of three separate experiments (ANOVA).  
720 **D**, cDNA from three explants of PBS-treated B16ova primary tumors (~0.3cm diameter) and  
721 three MRD B16ova cultures (derived from skin explants after regression with OT-I T-cell

722 therapy and growth for 72hrs in TNF $\alpha$ ) were screened by qrtPCR for expression the *ova* gene.  
723 Relative quantities of *ova* mRNA were determined (ANOVA). Statistical significance was set at  
724  $p < 0.05$  for all experiments. **E**,  $10^4$  parental B16 $ova$  cells; or **F**, MRD B16 $ova$  cells (derived as  
725 previously stated) were cocultured with purified CD8<sup>+</sup> OT-I T cells and/or purified NK cells from  
726 either wildtype C57BL/6 or from IL6 KO mice (OT-I:NK:Tumor 10:1:1) in triplicate in the  
727 presence or absence of anti-IL6. 72 hours later, supernatants were assayed for IFN $\gamma$  by ELISA.  
728 Mean and standard deviation of the triplicates are shown. Representative of three separate  
729 experiments. \*\*  $p < 0.01$  (ANOVA). **G**,  $10^4$  B16 $ova$  MRD cells (derived as already  
730 described) were cultured in triplicates, as in **F**. 72 hours later, cells were harvested and analyzed  
731 for intracellular IFN $\gamma$ . **H**, After 7 days of coculture, cDNA was screened by qrtPCR for  
732 expression of the *ova* gene. \*\*  $p < 0.01$ ; \*\*\*  $p < 0.001$  (ANOVA); Mean of each treatment is  
733 shown.

734 **Figure 6. Phenotyping of T cells.** Circulating lymphocytes from a tumor naïve C57BL/6 mice  
735 (left column) were compared to those from C57BL/6 mice treated and cleared of B16 primary  
736 tumors (right column) (n=2 mice per group, representative of four independent experiments).  
737 Multiparametric flow cytometry for live **A**, CD4<sup>+</sup> or CD8<sup>+</sup> T cells; **B and E**, The fraction of  
738 CD4<sup>+</sup> or CD8<sup>+</sup> cells that are CD62L<sup>hi</sup> or effector (CD62L<sup>lo</sup> CD44<sup>hi</sup>) phenotype. **C and F**, The  
739 fraction of CD62L<sup>hi</sup> CD4<sup>+</sup> or CD8<sup>+</sup> cells expressing the inhibitory receptors (IR) PD1 and TIM-  
740 3. **D and G**, The fraction of CD62L<sup>lo</sup> CD44<sup>hi</sup> effector cells expressing the IRs PD1 and TIM-3.  
741 To analyze quantitative flow cytometry data, one-way ANOVA testing was conducted with a  
742 Tukey post-test,  $p$  values reported from these analyses were corrected to account for multiple  
743 comparisons.

744 **Figure 7. Inhibition of tumor recurrence *in vivo*.** **A**, 5-day established subcutaneous B16tk  
745 tumors were treated with GCV i.p. on days 6-10 and 13-17. On day 27, mice with no palpable  
746 tumors were treated with control IgG, anti-asialo GM-1 (NK depleting), anti-TNF $\alpha$ , or anti-PD1  
747 every other day for three weeks and survival was assessed. Survival analysis was conducted  
748 using log-rank tests. The threshold for significance was determined by using the Bonferroni  
749 correction for multiple comparisons. Mice which developed a recurrent tumor were euthanized  
750 when the tumor reached a diameter of 1.0 cm. Eight mice per group, except for the GCV/anti-  
751 asialo GM-1 group n=9. \* $p$ <0.01 Representative of two separate experiments. **B**, Triplicate  
752 cultures of  $10^6$  splenocytes and LN cells from C57BL/6 mice were incubated with PBS, LPS (25  
753 ng/ml), or CpG for 48 hours, and supernatants were assayed for TNF $\alpha$  by ELISA. Mean and  
754 standard deviation of triplicates are shown; \*\*\* $p$ <0.0001 PBS vs LPS (t test). **C**, Cumulative  
755 results from skin explants at the sites of tumor from tumor-regressed mice treated with GCV  
756 (B16tk tumors), reovirus therapy (B16tk cells), or OT-I adoptive T-cell therapy (B16ova cells).  
757 Explants were cocultured with  $10^6$  splenocytes and LN cells from C57BL/6 mice in the presence  
758 of PBS, LPS, CpG, or LPS plus anti-TNF $\alpha$  (0.4 $\mu$ g/ml). 7 days later, adherent B16 tumor cells  
759 were counted and wells containing  $>10^4$  cells were scored for active growth of MRD cells.  
760  $P$ <0.001 LPS vs all other groups (ANOVA). **D**, 5-day established subcutaneous B16tk were  
761 treated with GCV i.p. on days 6-10 and 13-17 On days 27 and 29, mice with no palpable tumors  
762 were treated with LPS (25 $\mu$ g/injection). Mice were treated in-parallel with control IgG, anti-  
763 asialo GM-1, anti-TNF $\alpha$ , or anti-PD1 every other day for three weeks. Mice with recurrent  
764 tumors were euthanized when the tumors reached a diameter of 1.0 cm. Survival of mice with  
765 time is shown. \*\* $p$ <0.01; \*\*\*  $p$ <0.001. Survival analysis was conducted using log-rank tests.

766 The threshold for significance was determined by using the Bonferroni correction for multiple  
767 comparisons. Representative of two experiments.

768

769

770

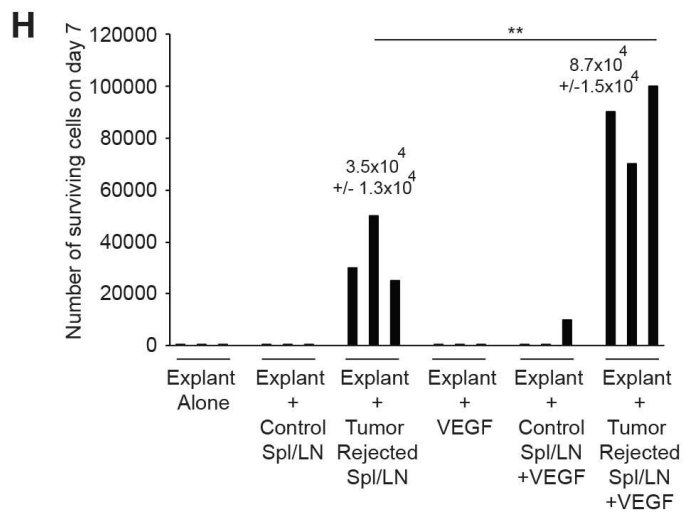
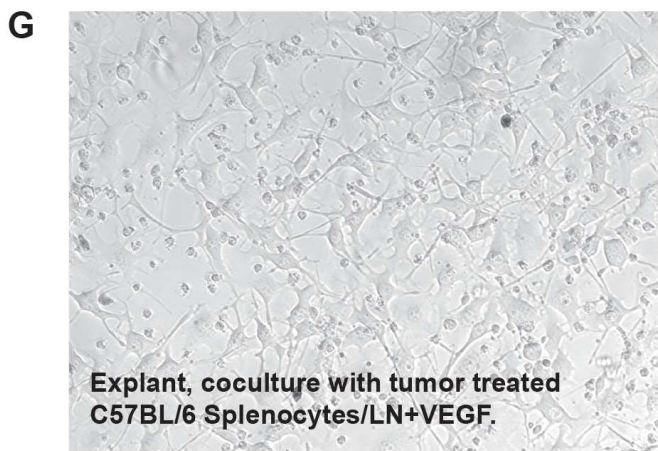
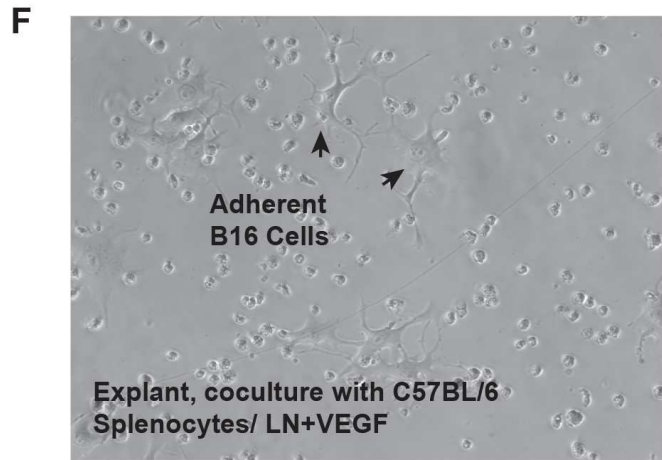
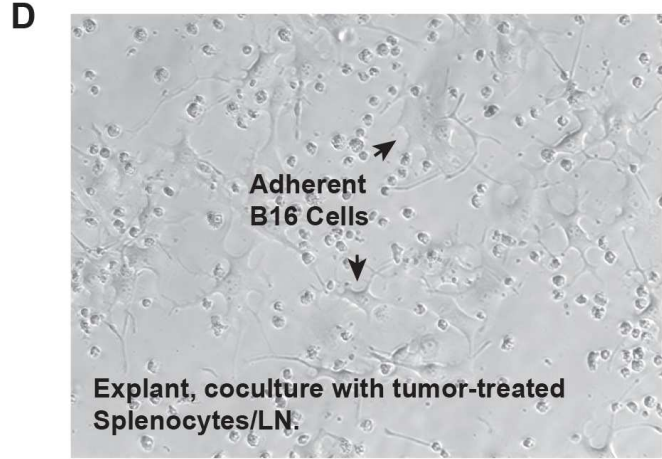
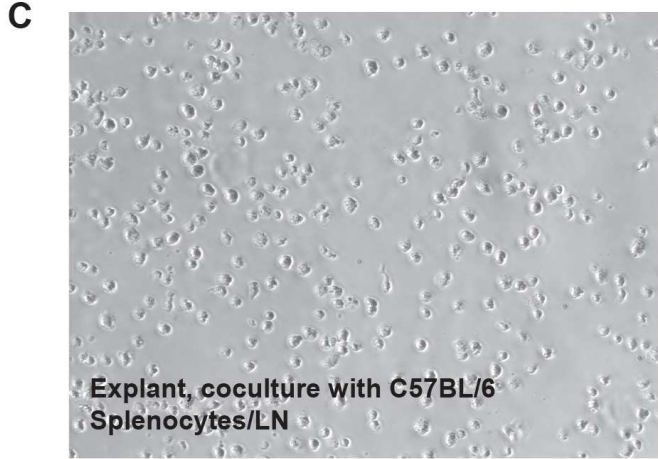
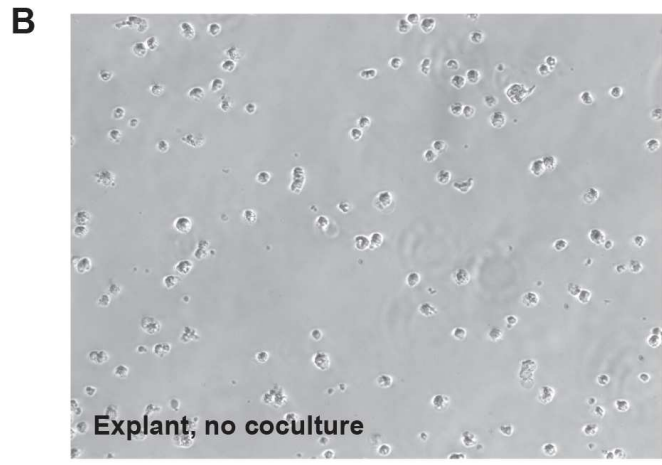
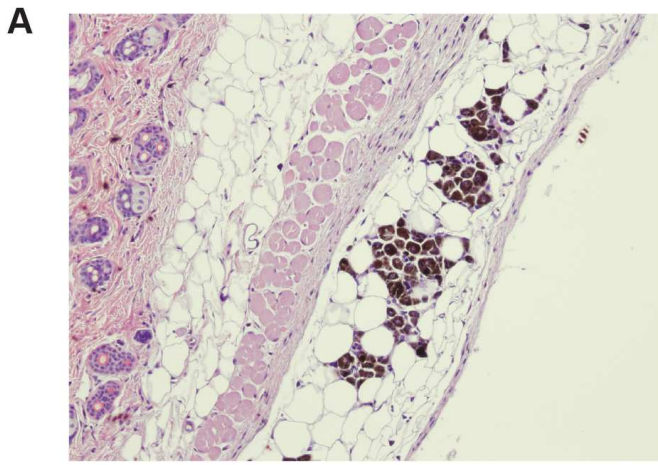
Table 1

Culture Conditions	Rate of Outgrowth >10 <sup>4</sup> cells on d7
Explant alone	2/19
Explant + Control Spl/LN	0/7
Explant + Tumor Rejected Spl/LN	4/6
Explant + VEGF	0/4
Explant + Control Spl/LN + VEGF	2/5
Explant + Tumor Rejected Spl/LN + VEGF	4/4

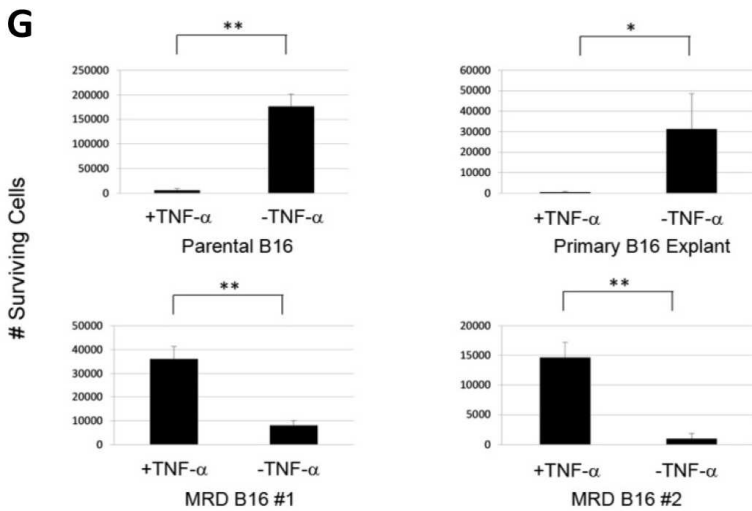
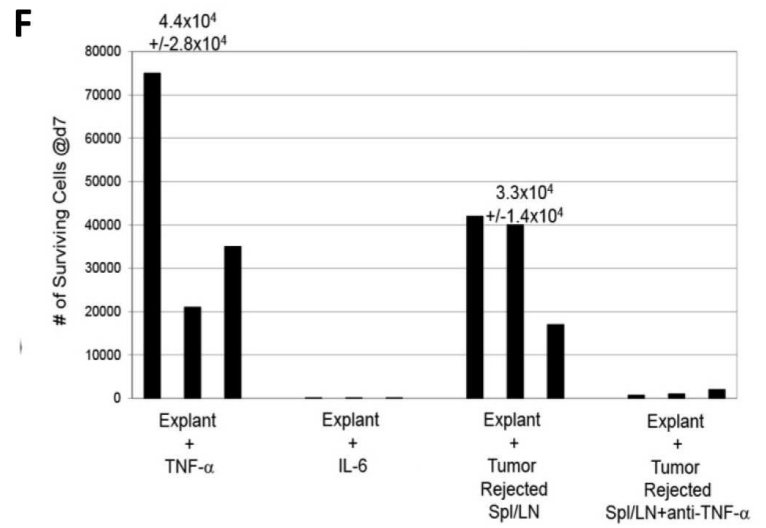
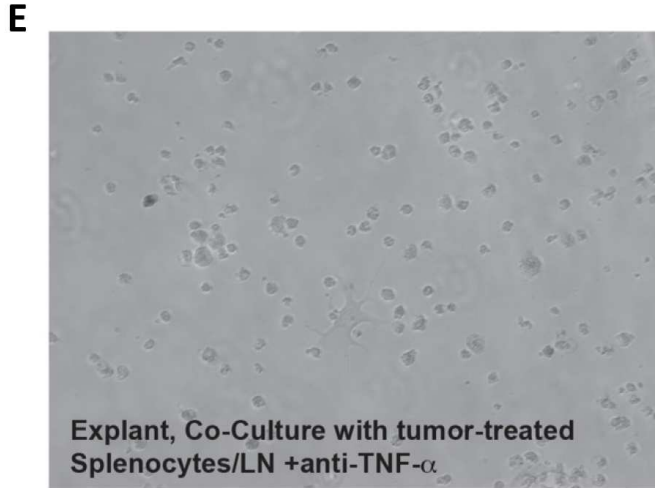
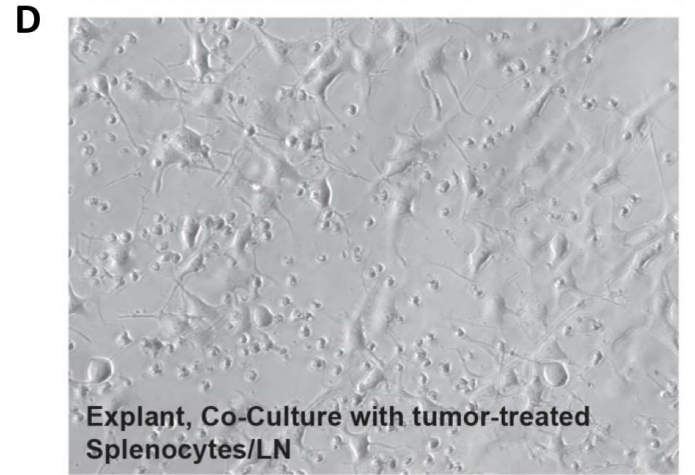
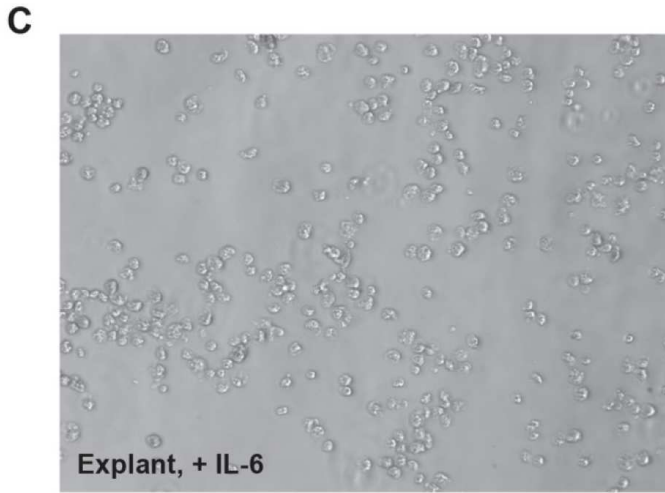
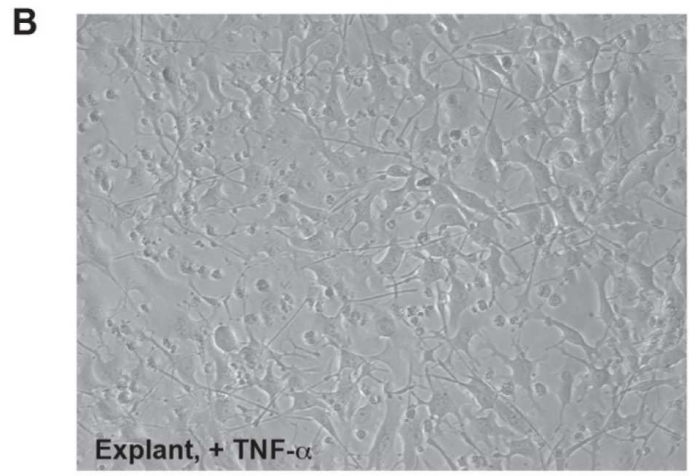
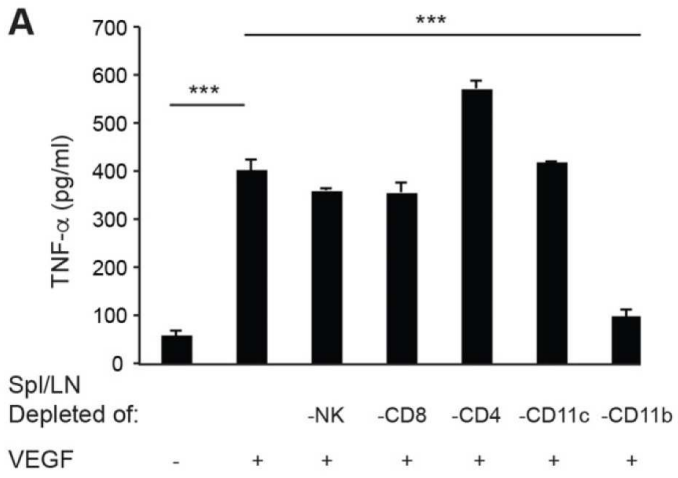
\* MRD explants from any of 4 different primary treatments.

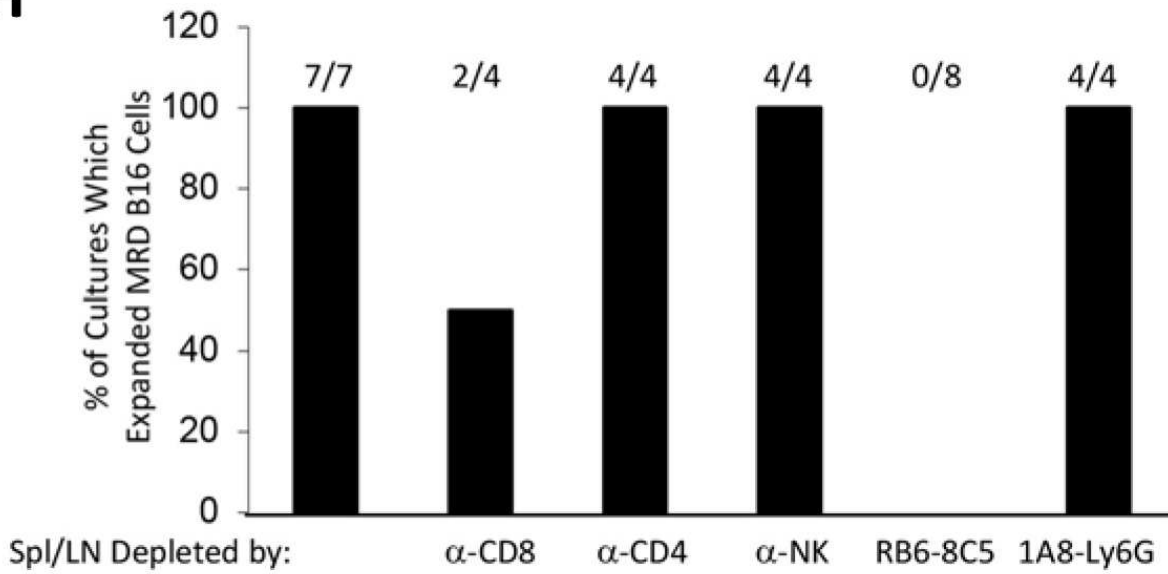
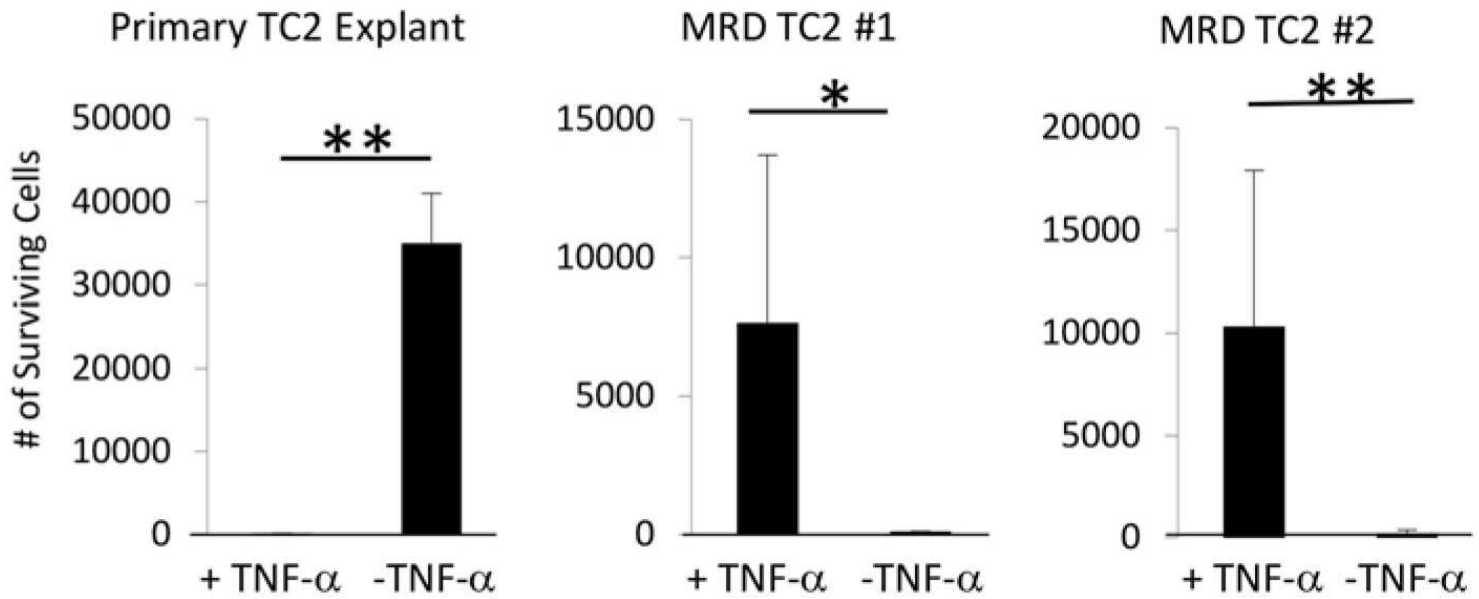
Table 2

Frontline Therapy Inducing MRD	Viable Cultures of B16 MRD	
	-TNF- $\alpha$	+TNF- $\alpha$
B16tk/GCV	0/7	5/5
B16tk/i.t. Reovirus	1/9	4/4
B16ova/OT-I	0/7	5/7
B16tk/Pmel/ VSV-hgp100	1/4	3/3
<b>TOTAL</b>	<b>2/27</b> <b>(7%)</b>	<b>17/19</b> <b>(89%)</b>



**Figure 1**



**H****I**

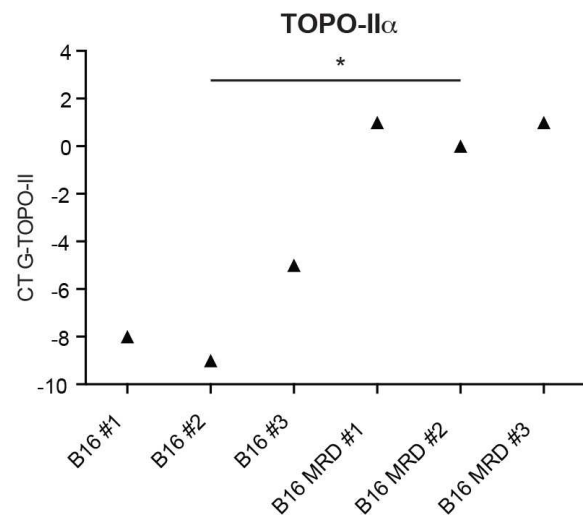
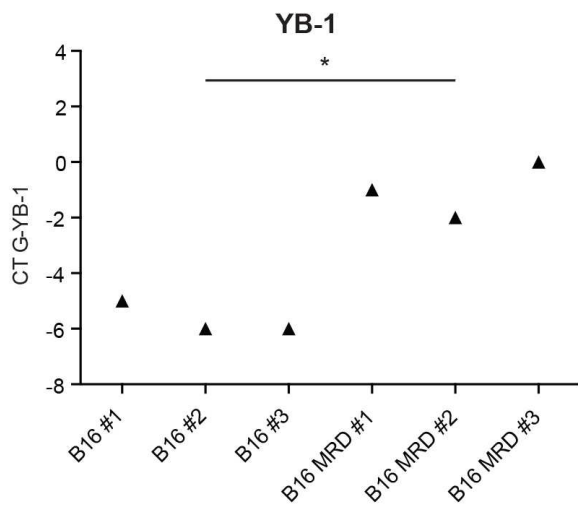
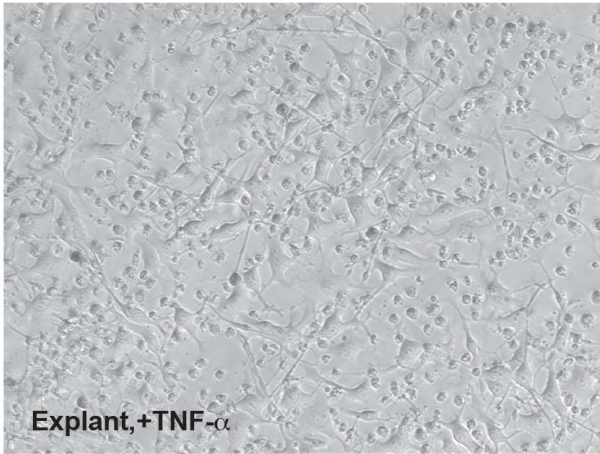
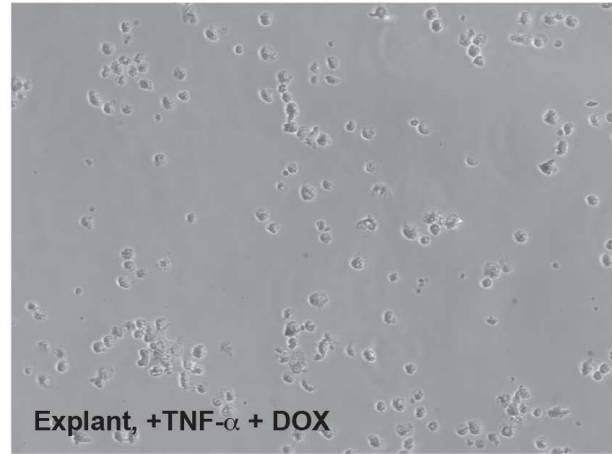
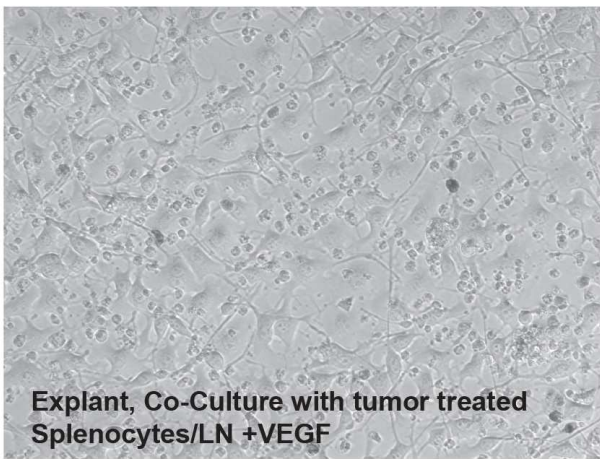
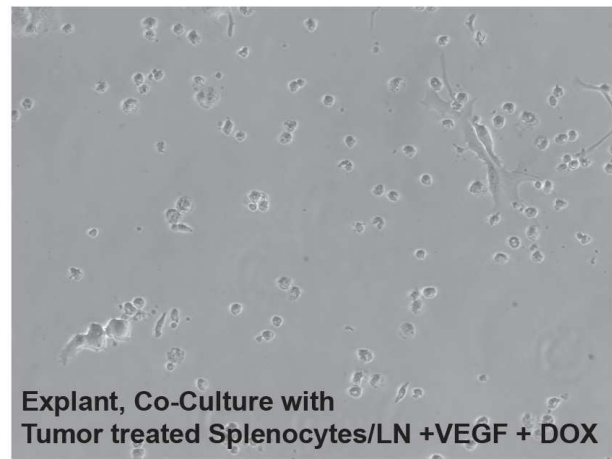
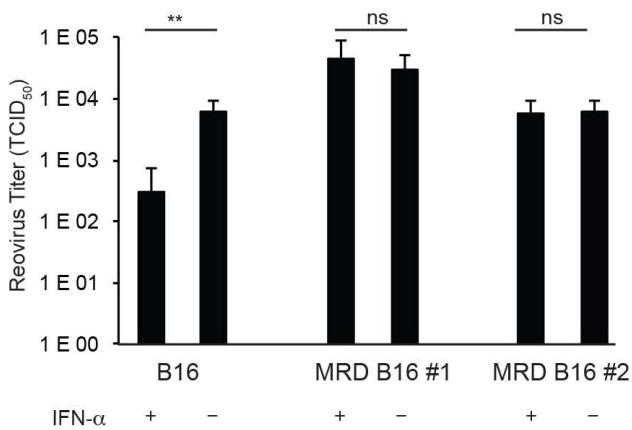
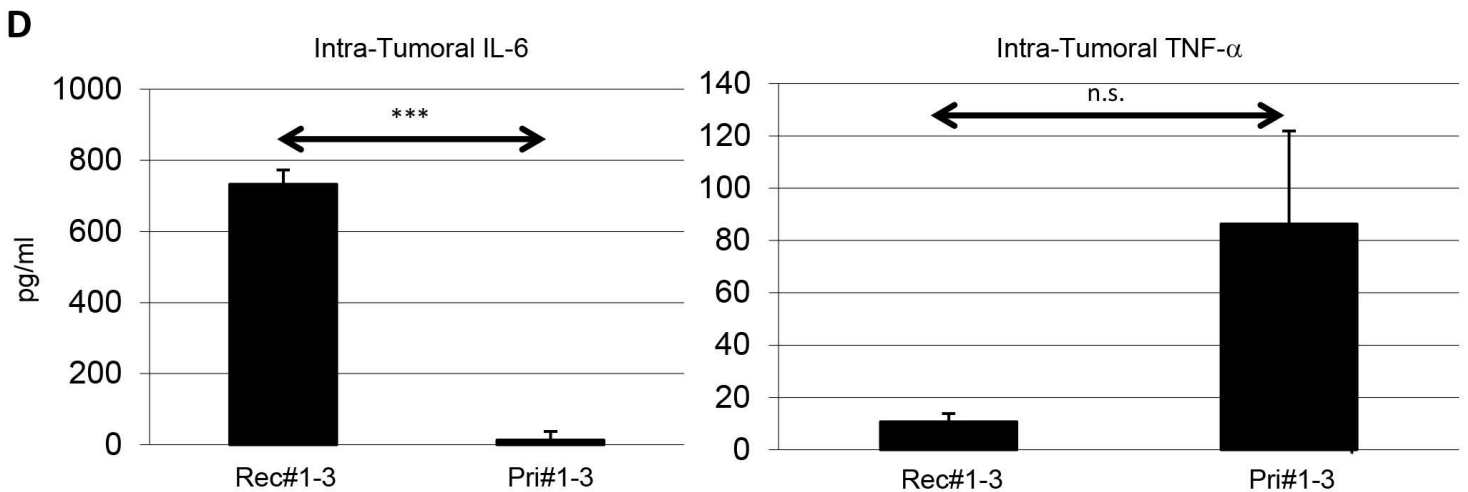
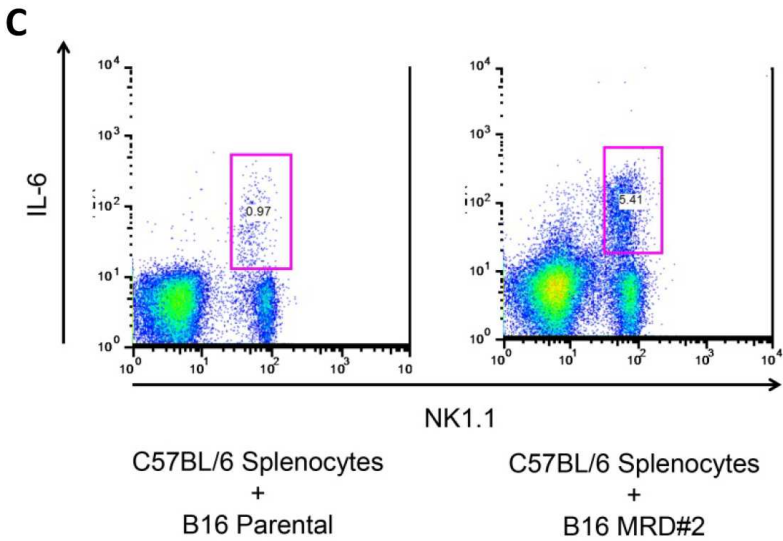
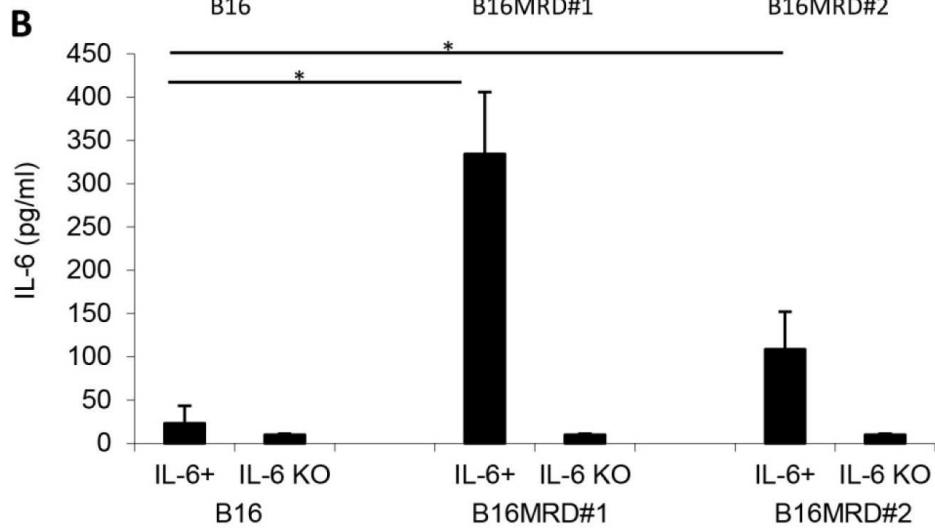
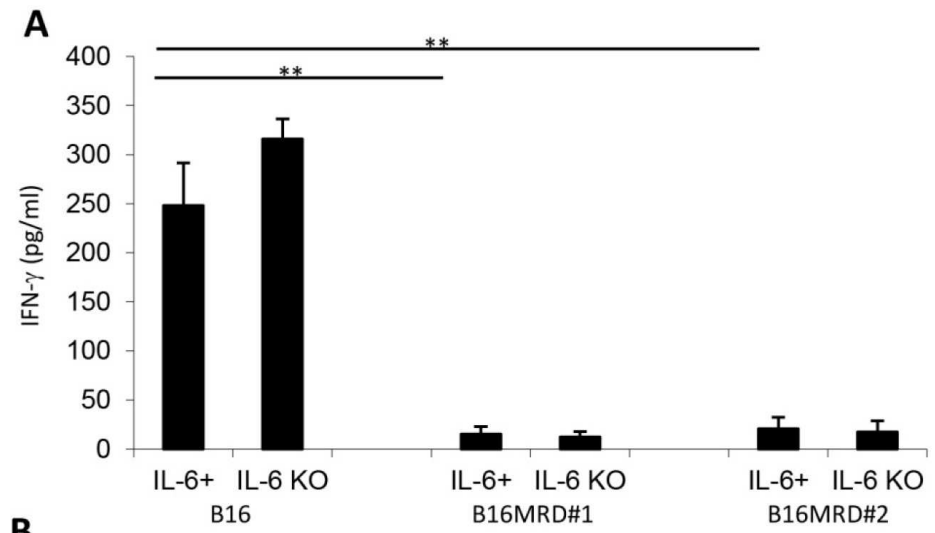
**A****B****C****D****E****F****Figure 3**

Figure 4



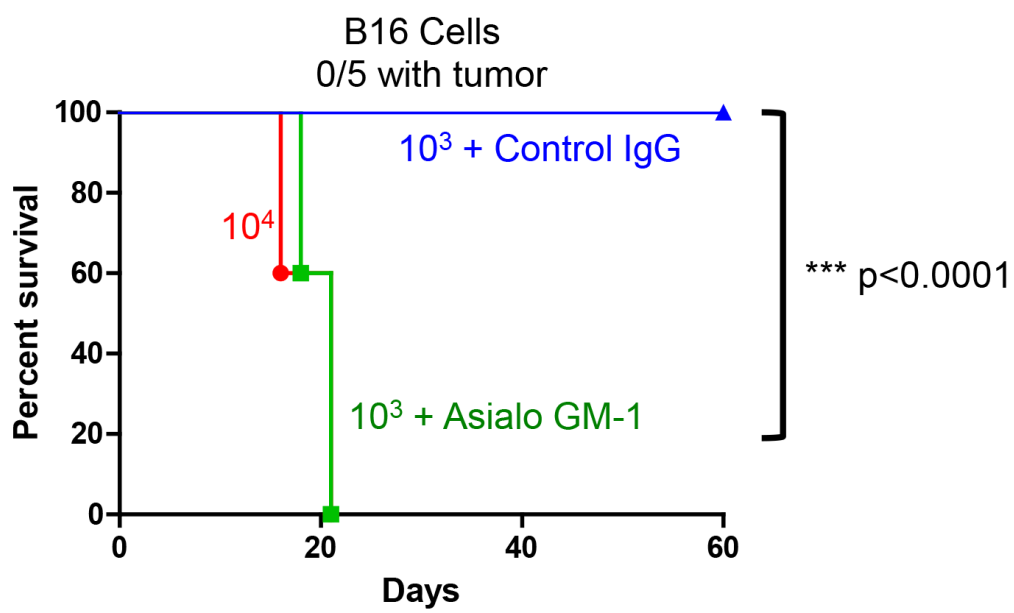
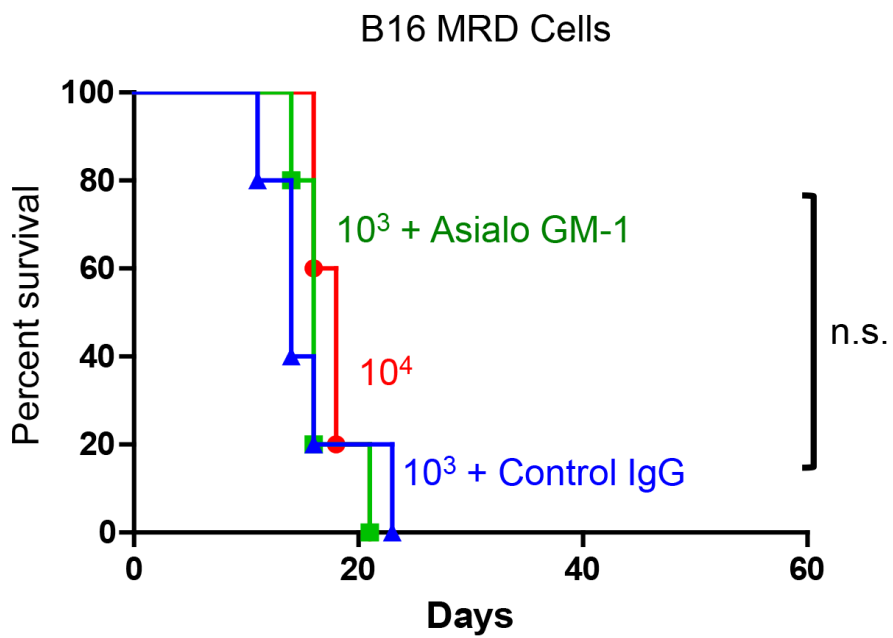
**E****F**

Figure 4

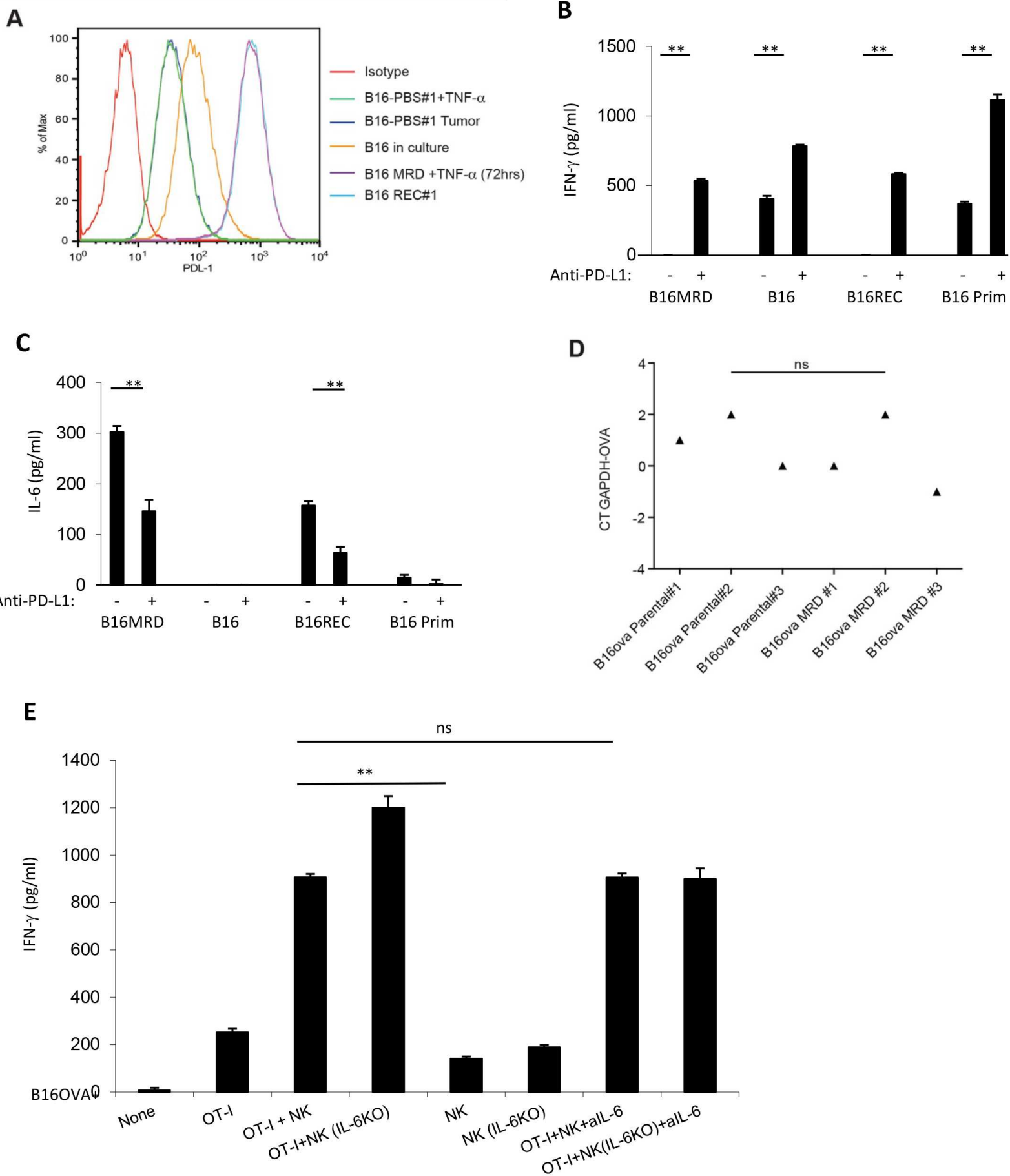


Figure 5

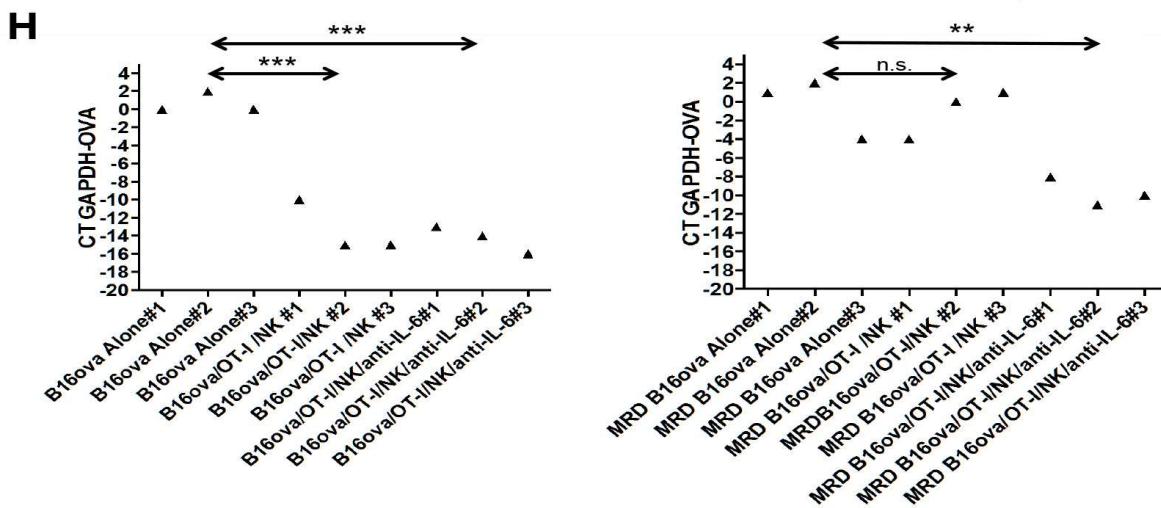
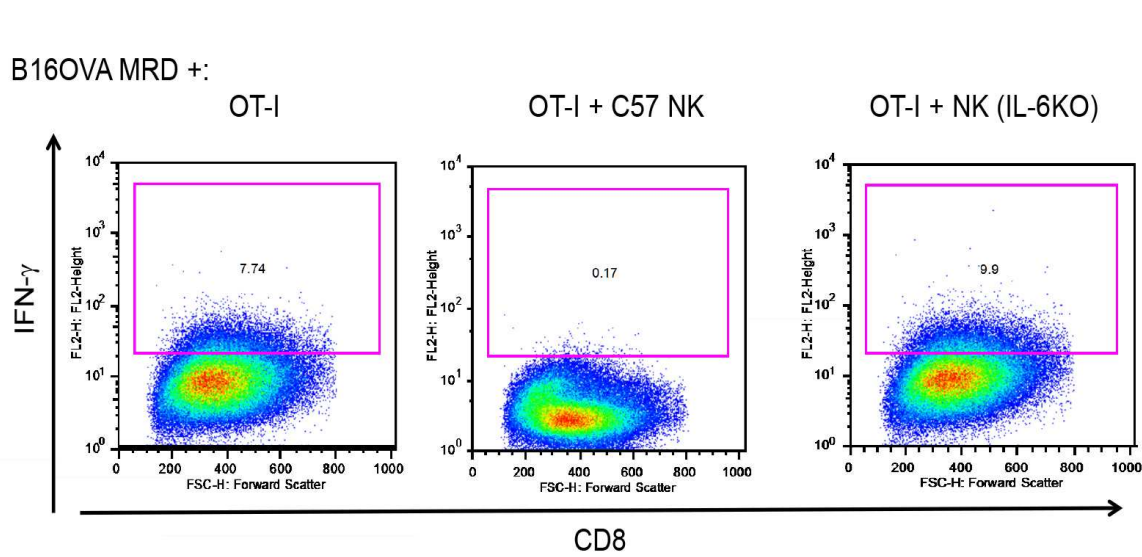
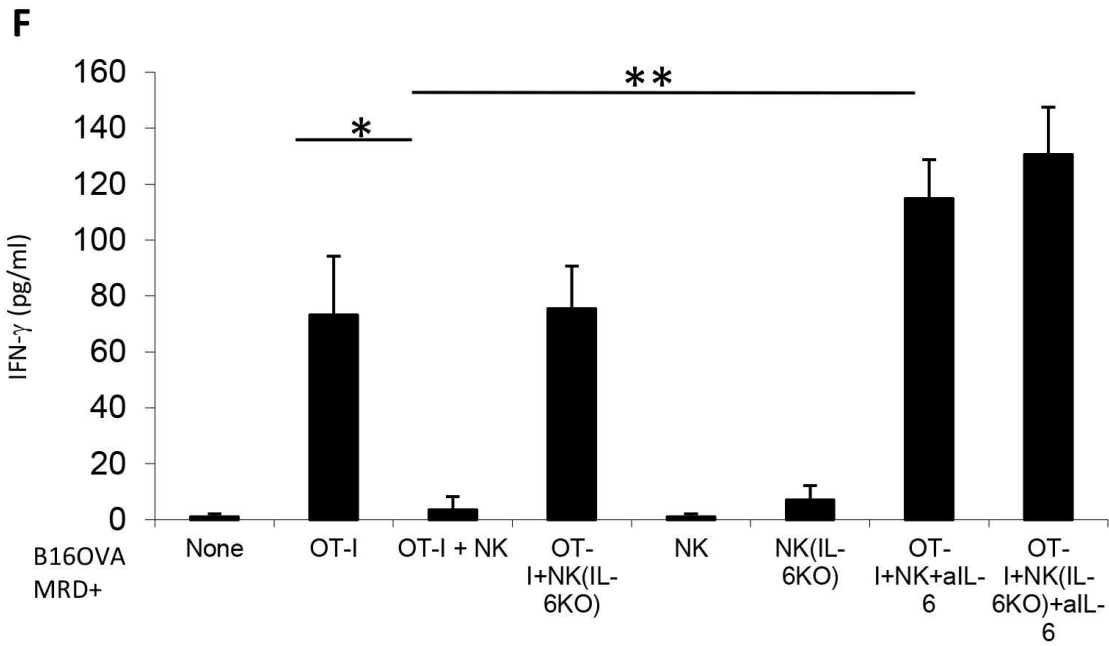
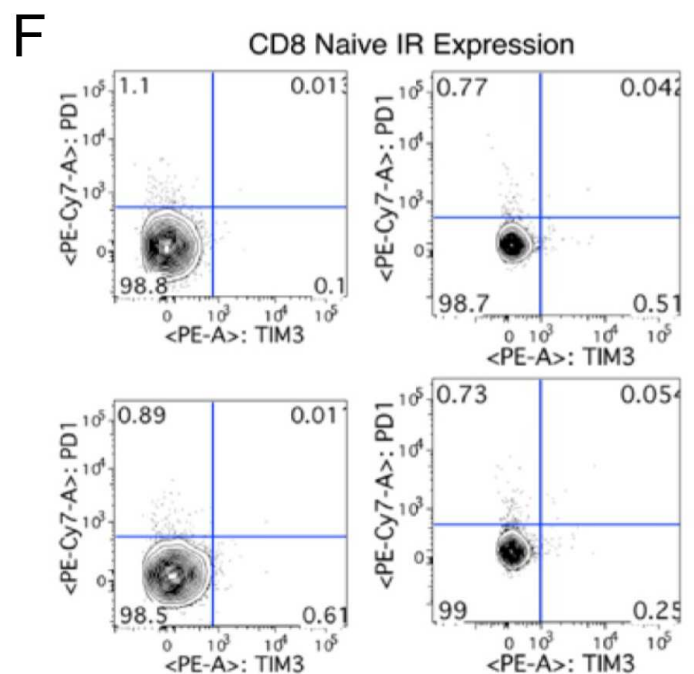
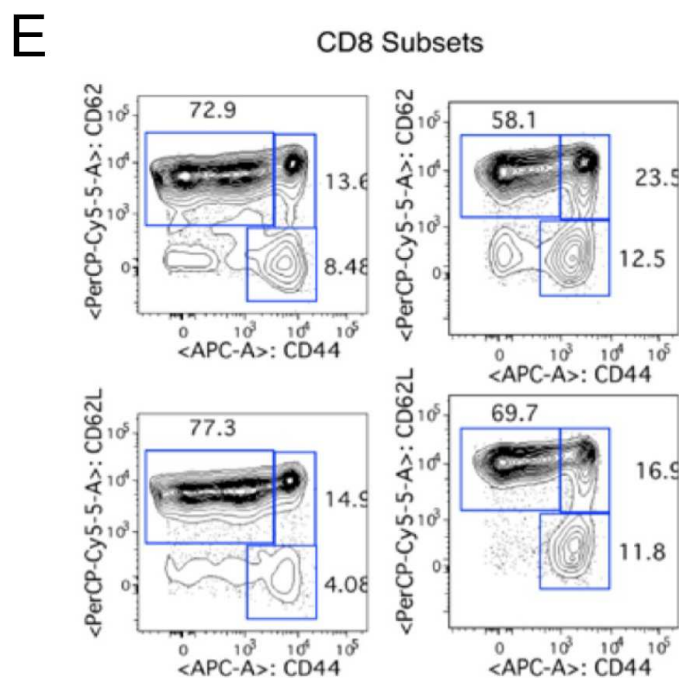
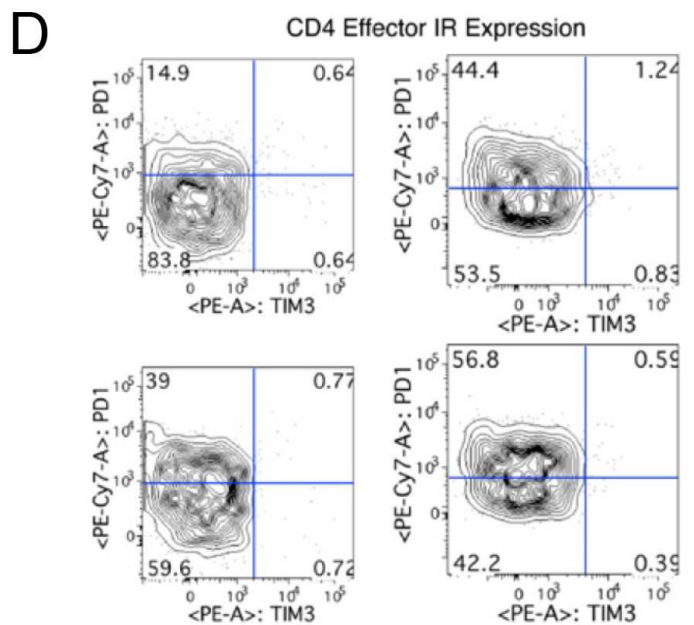
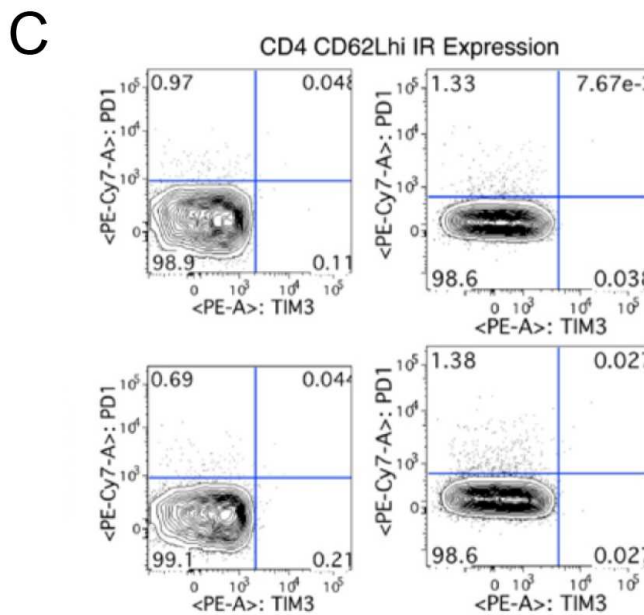
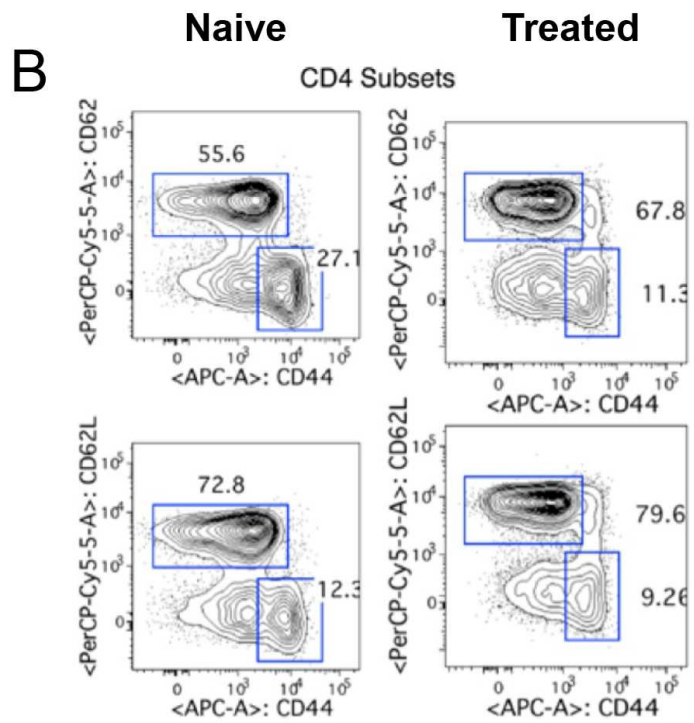
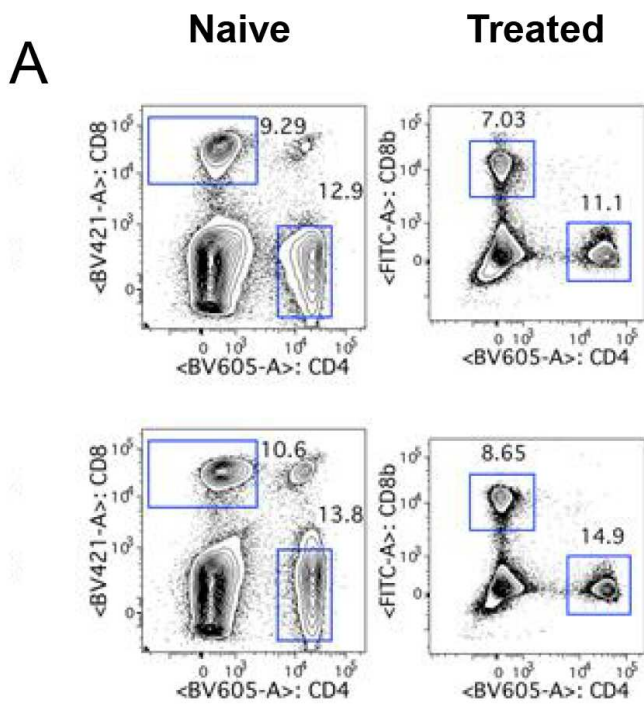


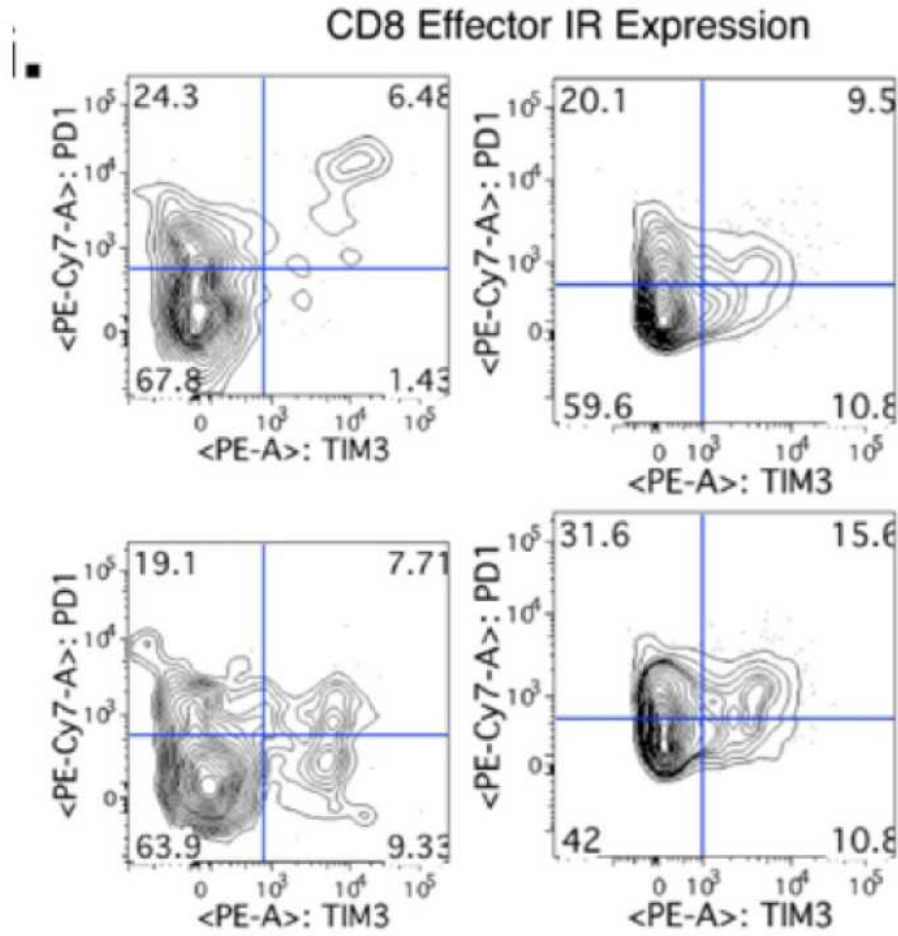
Figure 5



# G

## Naive

## Treated



### Mouse 1

### Mouse 2

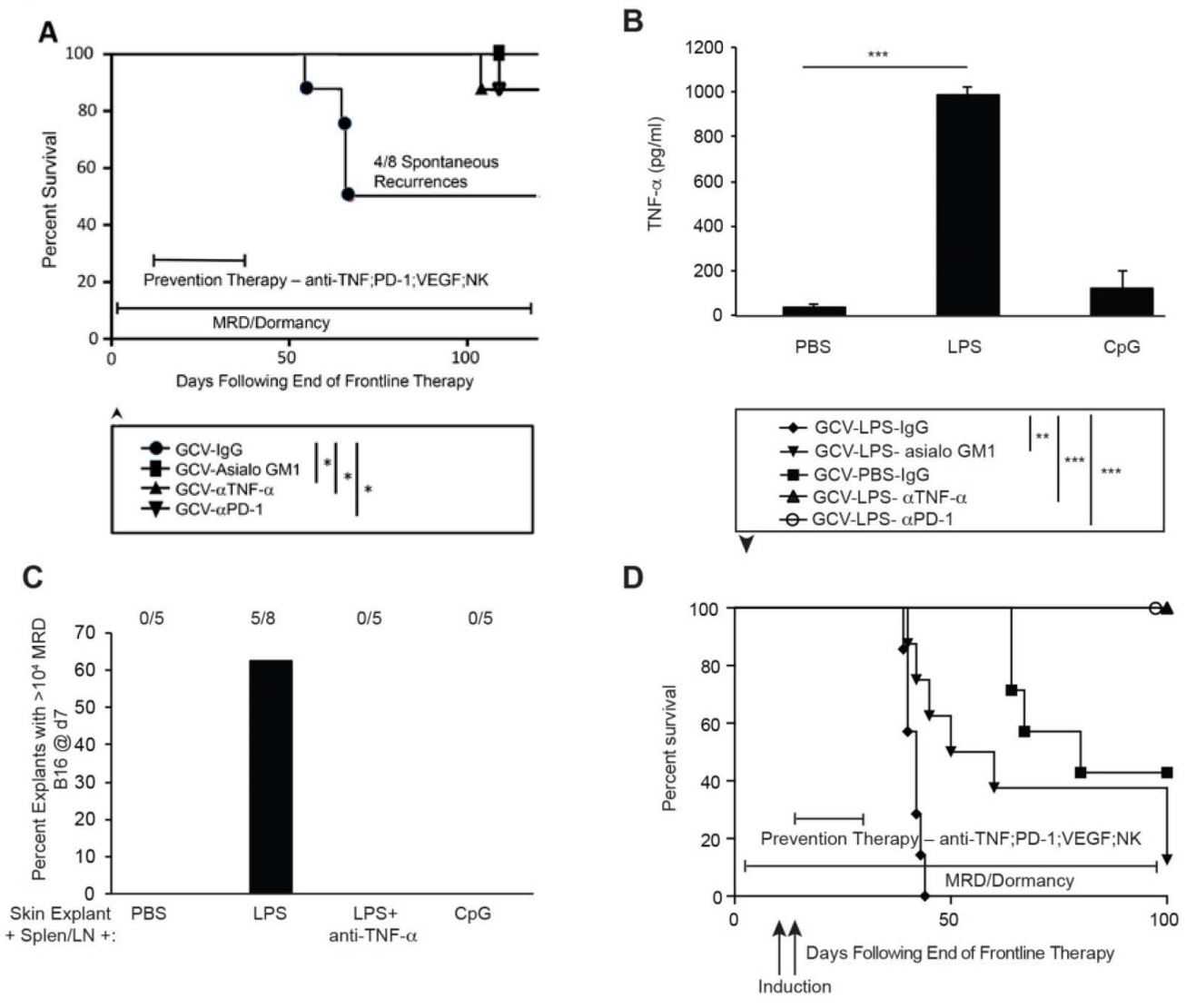


Figure 7